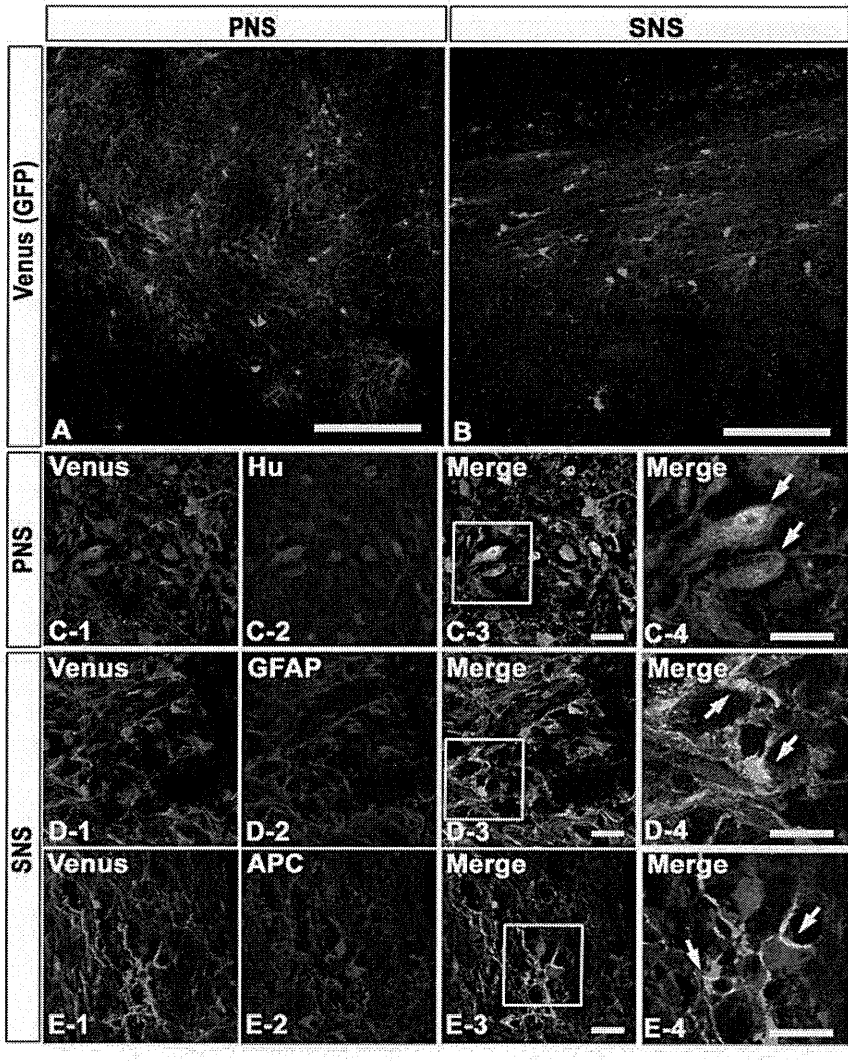

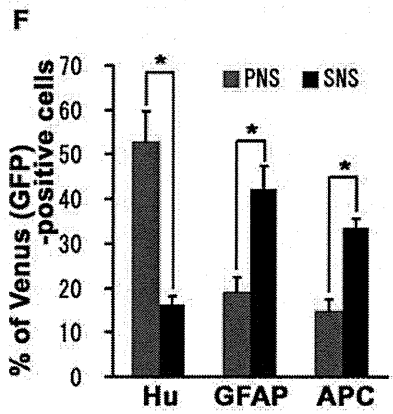

Figure 4. ***In vivo*** **differentiation characteristics of PNS and SNS grafted onto the injured spinal cord.** (A)(B) Venus-positive PNS- and SNS-derived grafted cells integrated at or near the lesion epicenter. Venus expression was detected by immunohistochemistry using an antibody against GFP. Scale bar 100 μm. (C)(D)(E) Representative immunohistochemical images of Venus-positive grafted cells that were positive for markers of neural lineages: Hu-positive neurons from PNS group (C), GFAP-positive astrocytes from SNS group (D), and APC-positive oligodendrocytes from SNS group (E). Scale bar: 20 μm. (C-4, D-4, E-4) Higher-magnification image of the boxed areas in C-3, D-3, E-3. Scale bar: 20 μm. (F) The percentage of cell type-specific marker positive cells among the Venus-positive grafted cells, showing the *in vivo* differentiation characteristics of PNS and SNS. The percentage of Hu-positive neurons in the PNS group (52.8±19.1%) was three times that in the SNS group (16.3±5.2%). In contrast, the percentage of GFAP-positive astrocytes or APC-positive oligodendrocytes in the SNS group (42.2±14.4, 33.6±5.4%) was twice that in the PNS group (19.0±9.3, 14.8±7.1%). Values are means ± s.e.m. ($n=4$). *: $P<0.05$, PNS vs. SNS.
doi:10.1371/journal.pone.0007706.g004

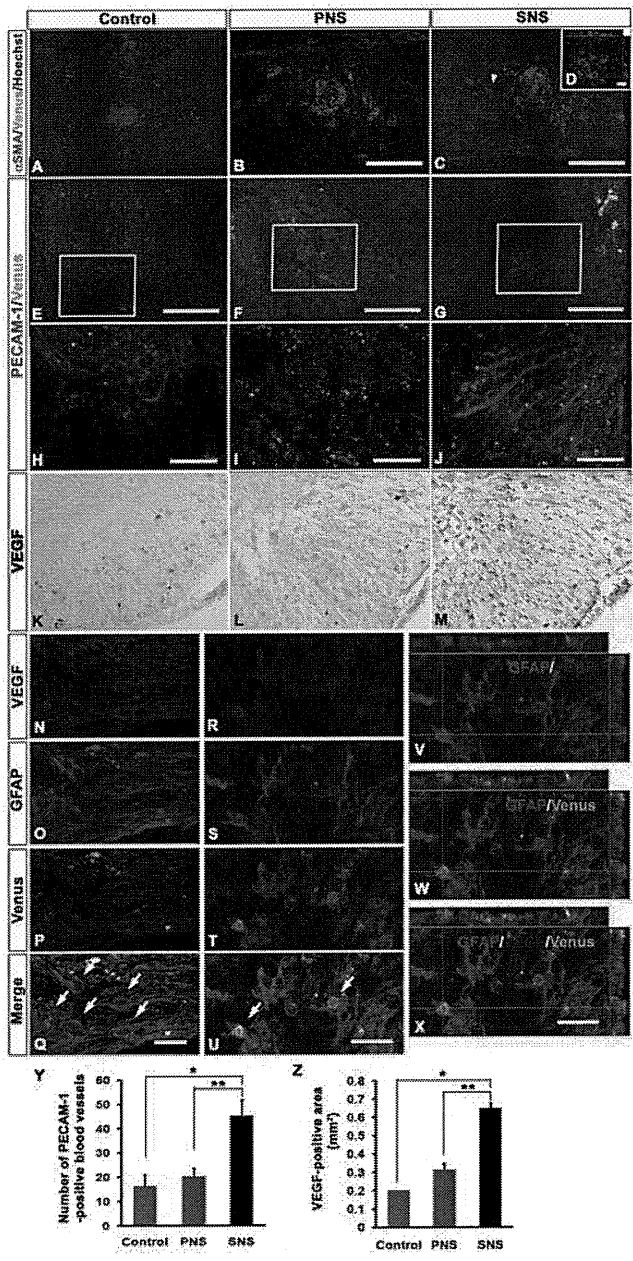

Figure 5. Transplanted SNS, but not PNS, enhanced angiogenesis after SCI. (A)(B)(C) Representative images of αSMA-immunostained sections obtained from the control (A), PNS (B), and SNS (C) groups. Scale bar: 500 μm. (D) Higher-magnification image of the area indicated by the arrowhead in C. Scale bar: 20 μm. While a few αSMA-positive Venus-expressing grafted cells were observed at and near the lesion site in sagittal sections of both the control and PNS groups, significantly more αSMA-positive cells were found in the SNS group, with Venus-positive grafted cells accumulated near the αSMA-positive cells, not colocalized with them. (E)(F)(G) Representative images of PECAM-1-immunostained sections obtained from the Control (E), PNS (F), and SNS (G) groups. Scale bar: 200 μm. (H)(I)(J) Higher-magnification images of the boxed areas in E, F, and G. Scale bar: 100 μm. (K)(L)(M) Representative images of axial sections stained for vascular endothelial growth factor (VEGF). Scale bar: 100 μm. (N–X) Expression of VEGF in GFAP-positive astrocytes among host-derived cells (N–Q) and Venus-positive (GFP immunostained) graft-derived cells (R–X) in the spinal cord from the SNS group (arrows indicate VEGF/GFAP double-positive cells). SNS transplants promoted VEGF expression in both the host- and graft-derived GFAP-positive astrocytes. Scale bar: 20 μm. (Y) Quantitative analysis of blood vessels at the lesion epicenter. PECAM-1 immunostaining revealed similar results, with significantly more PECAM-1-positive blood vessels observed at the lesion site in the SNS group compared with the PNS and control groups. Values are means ± s.e.m. (n = 3).*: $P<0.05$, Control vs. SNS. **: $P<0.05$, PNS vs. SNS. (Z) Quantitative analysis of the VEGF-positive area at the lesion epicenter. The VEGF-positive area at the lesion epicenter was significantly broader in the SNS group than in the other groups. Values are means ± s.e.m. (n = 3).*: $P<0.05$, Control vs. SNS. **: $P<0.05$, PNS vs. SNS.

doi:10.1371/journal.pone.0007706.g005

rim of the lesion epicenter in the control and PNS groups, there were significantly more NF-H-positive neuronal fibers in the SNS group at the lesion epicenter and perilesional area (Fig. 6**A, B, and E**). 5-HT-positive serotonergic fibers, which are descending raphespinal tract axons [16,17], were observed at the sites caudal to the lesion epicenter in all three groups 6 weeks after injury (Fig. 6**C**). Quantitative analysis revealed that there were significantly more 5-HT-positive fibers at the site 4 mm caudal to the lesion epicenter (Th10 level), which was approximately at the L1 level, in the SNS group compared with the other groups (Fig. 6F).

While few GAP43-positive axons [18,19,20] were detected caudal to the lesion epicenter in the control and PNS groups, there were significantly more GAP43-positive fibers in the SNS group in the ventral region 1 mm caudal to the lesion epicenter (Fig. 6**D, G**), suggesting that transplantation of the gliogenic SNS, but not of the neurogenic PNS, promoted axonal regeneration in the injured spinal cord.

We also observed NF-H-positive neuronal fibers extending along with the GFAP-positive immature astrocytes, which may have been partially derived from the grafted Venus-positive cells, and crossing the perilesional area in the SNS group (Fig. 7**A and B**). Furthermore, the SNS-derived Venus-positive cells differentiated into MBP-positive oligodendrocytes, which myelinated NF-H-positive fibers (Fig. 7**C**). Electron microscopy also revealed active remyelination in the SNS group (Fig. 7**D–F**). The grafted cells were in small groups containing 50–100 cells (Fig. 7**D**). The axons at these sites were enwrapped by myelin sheathes of various thicknesses and numbers of lamellae, which were contributed by the grafted cells, as confirmed by immunolabeling with an anti-GFP antibody to distinguish the transplanted cells from the locally surviving recipient cells (Fig. 7**E**). A much higher magnification revealed nanogold-labeled Venus-positive spots in the outer and inner mesaxons of the myelin cytoplasm. Some axons close to the lesion epicenter had undergone considerable re-myelination, and were enwrapped in spirals of more than ten layers of compacted lamellae (Fig. 7**F**).

Finally, we monitored the locomotor functional recovery in all three groups using the BMS scoring scale [21]. The contusive SCI resulted in complete paralysis (BMS score 0) on day 1, followed by gradual recovery with a plateau around 3 weeks. Although there was no significant difference in the BMS scores among the control, PNS, and SNS groups on day 14, the SNS group exhibited significantly better functional recovery than the PNS and control groups on day 21 and thereafter. On the other hand, there was no significant difference in the BMS scores between the PNS and control groups (Fig. 7**G**). From a clinical perspective, the recovery of the SNS group to levels exhibiting frequent to consistent weight-supported plantar steps and occasional forelimb-hindlimb coordination was especially noteworthy.

Discussion

Methods for effectively inducing neural differentiation from pluripotent ES cells have been extensively studied [6] and are

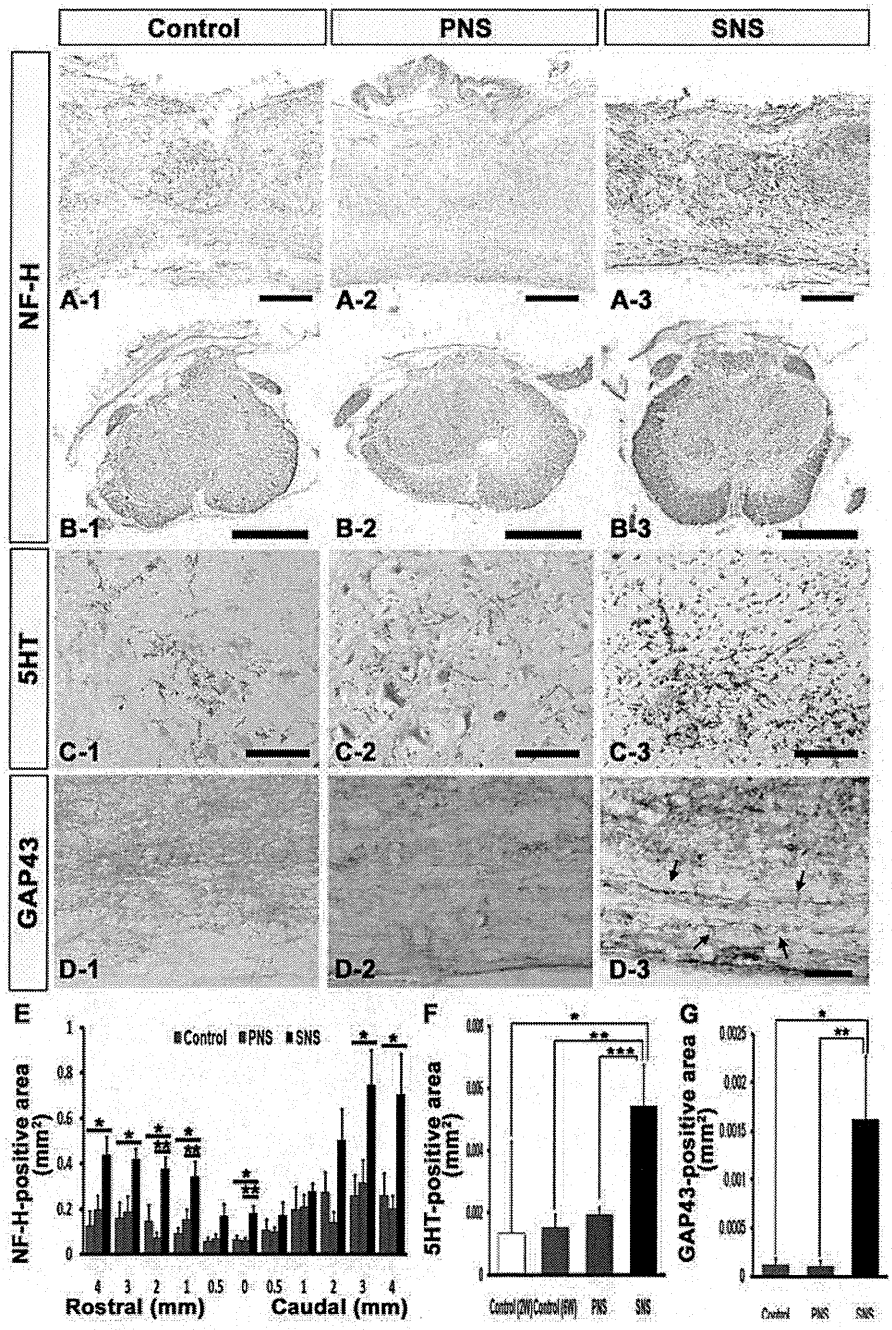

Figure 6. Transplanted SNS, but not PNS, promoted axonal growth. (A) Representative images of sagittal sections stained for NF-H in all three groups. Scale bar: 200 μm. (B) Representative images of axial sections stained for NF-H at the lesion epicenter in all three groups. Scale bar: 500 μm. (C) Representative images of axial sections stained for 5-HT 4 mm caudal to the epicenter from all three groups. Scale bar: 100 μm. (D) Representative images of midsagittal sections stained for GAP43 in the ventral region 1 mm caudal to the epicenter from all three groups, and intact spinal cord. Arrows: GAP43-positive fibers. Scale bar: 50 μm. (E) Quantitative analysis of the NF-H-positive area at each distance point. While few NF-H-positive neuronal fibers were observed at the rim of the lesion epicenter in both the control and PNS groups, there were significantly more NF-H-positive neuronal fibers in the SNS group (B-3) at the lesion epicenter, 1, 2, 3, 4 mm rostral and 3, 4 mm caudal to the lesion epicenter compared with the control group (B-1), and at the lesion epicenter and 1, 2 mm rostral to the lesion site compared with the PNS group (B-2). Values are means ± s.e.m. ($n = 5$). *: $P<0.05$, Control vs. SNS. **: $P<0.05$, PNS vs. SNS. (F) Quantitative analysis of the 5-HT-positive area in axial sections 4 mm caudal to the lesion epicenter. Significantly more 5-HT-positive fibers were observed in the SNS group compared with the other groups. Values are means ± s.e.m. ($n = 3$).*: $P<0.05$, Control (2 weeks after injury) vs. SNS. **: $P<0.05$, Control (6 weeks after injury) vs. SNS. ***: $P<0.05$, PNS vs. SNS. (G) Quantitative analysis of the GAP43-positive area in midsagittal sections in the ventral region 1 mm caudal to the epicenter. Significantly more GAP43-positive fibers were observed in the SNS group than in the other groups. Values are means ± s.e.m. ($n = 4$). *: $P<0.05$, Control vs. SNS. **: $P<0.05$, PNS vs. SNS.

doi:10.1371/journal.pone.0007706.g006

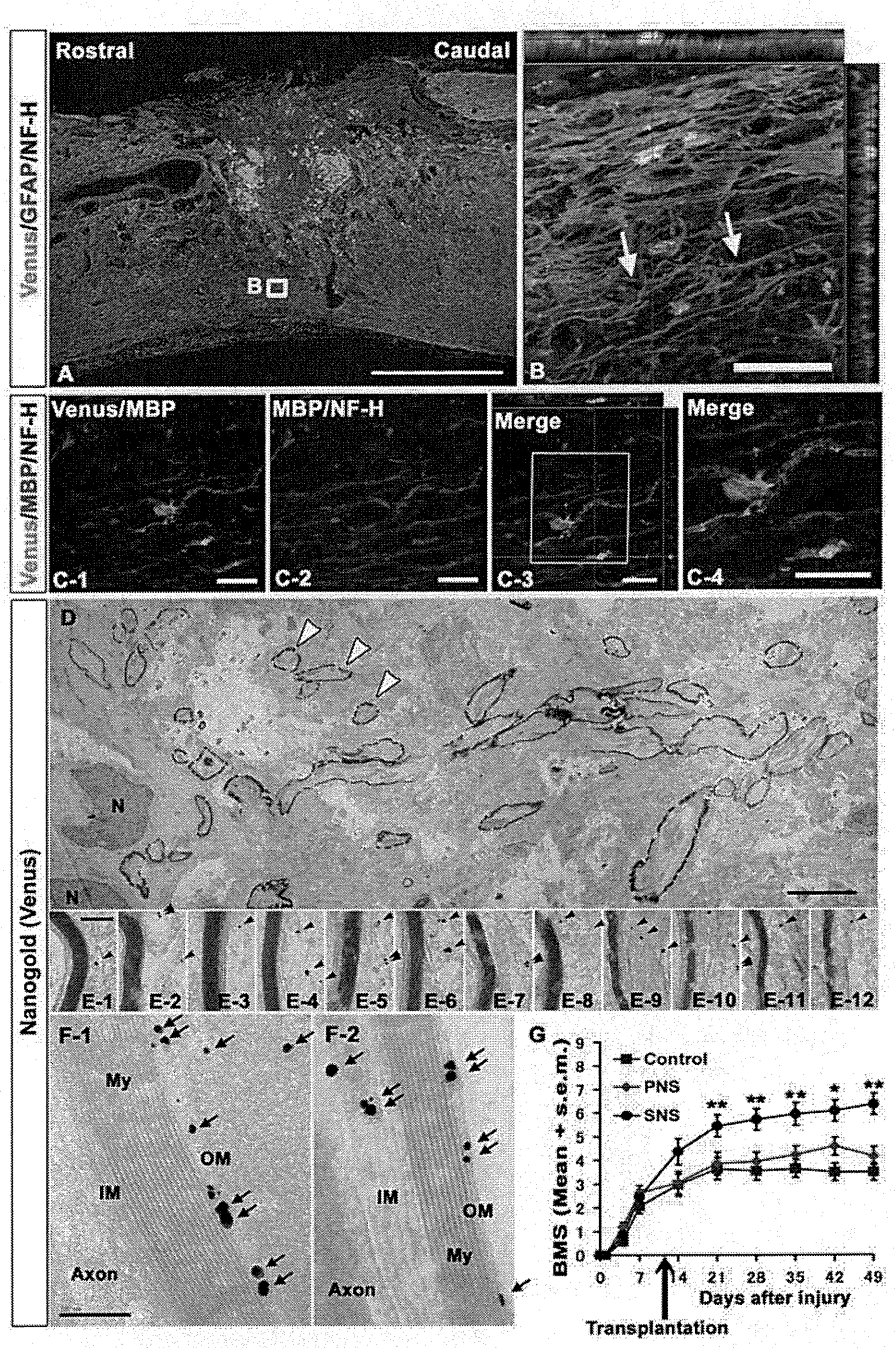

Figure 7. Transplanted SNS, but not PNS, promoted axonal growth, remyelination and functional recovery. (A) NF-H-positive neuronal fibers were observed along with GFAP-positive immature astrocytes derived either from the Venus-positive grafts or the host, and crossed the perilesional area in the SNS group. Scale bar: 50 μm. (B) Higher magnification images of the boxed area in A. Arrows: some examples of axons associated with Venus (GFP)-positive astrocytes. (C) Immunohistochemical analysis of MBP and NF-H in the SNS-transplanted injured spinal cord. SNS-derived Venus-positive cells differentiated into MBP-positive oligodendrocytes, which myelinated NF-H-positive fibers. Scale bar: 20 μm. (D)(E)(F) Representative electron-microscopic images of a remyelination site in sagittal sections from injured spinal cords grafted with SNS, which were immunostained for Venus (grafted cells) using an anti-GFP antibody. Low-magnification images show a group of grafted cells with active remyelination (some indicated by open arrowheads) (D). High-magnification images from (E-1) to (E-12) were obtained from (D), and show various numbers of lamellae in the myelin sheath. The remyelinating transplanted cells were detected as black dots (arrowheads). Venus (GFP)-positive dots (arrows) were localized to the outer and inner mesaxons of the myelin cytoplasm (OM, IM) (F). My: Myelination, N: Nucleus, Scale bar: 5 μm for D, 200 nm for E and F. (G) Mean Basso Mouse Scale for Locomotion (BMS) scores for each group over the 49-day recovery period. Although there was no significant difference in the BMS scores among the control, PNS, and SNS groups on day 14, the SNS group exhibited significantly better functional recovery than the PNS and control groups on day 21 and thereafter. On the other hand, there was no significant difference in the BMS scores between the PNS and control groups. Values are means ± s.e.m. ($n = 11$), *: $P<0.05$, SNS vs. control, 42 days after injury. **: SNS vs. PNS or SNS vs. control on day 21, 28, 35, and 49 after injury.

doi:10.1371/journal.pone.0007706.g007

expected to be applied in cell replacement therapies for SCI [22]. However, detailed investigations of the optimal cell sources for promoting recovery from SCI are lacking. We recently developed an ES cell culture system that recapitulates the temporal progression of NS/PCs from the FGF-responsive early neurogenic NS/PCs to the EGF-responsive late gliogenic NS/PCs, consistent with CNS development *in vivo* [10,23] (Fig. 1**G, H**). Taking advantage of this difference in differentiation tendency, here we examined the distinct effects of the neurogenic PNS and gliogenic SNS on recovery following SCI.

One of the mechanisms underlying this developmental stage-dependent gliogenic transition of NS/PCs is the epigenetic regulation of glial cell-specific genes. The gradual demethylation of CpGs around the Stat3 recognition sequence in the GFAP promoter is thought to be involved in the developmental stage-dependent increase in transcription of the GFAP gene and the acquisition of astrocytic differentiation potentials [24,25,26]. Interestingly, this process is also observed in our ES cell-derived neurosphere system, in which the proportion of unmethylated CpGs in this region gradually increases during the development of ES cells into secondary neurospheres [10]. This may explain why the *in vitro* differentiation potentials of both the PNS and SNS were preserved even after their transplantation into injured spinal cord, despite its gliogenic environment (Fig. 4**A–F**) [27]. Since there was no significant difference in the numbers of grafted PNS and SNS in the injured spinal cord 6 weeks after transplantation, the difference in the in vivo differentiation potentials of the grafted neurospheres was the critical factor influencing the functional recovery after SCI. More than 70% of the grafted SNS cells differentiated into GFAP-positive astrocytes or APC-positive oligodendrocytes, and the engraftment of these cells led to improved functional recovery (Fig. 4**F**). In contrast, engrafted PNS cells, which mainly differentiated into neurons, did not promote functional recovery.

Determining the exact mechanisms through which the transplanted SNS, or glial cells, improved the recovery of the traumatically injured CNS has been challenging. The engrafted SNS cells could promote a wide range of effects, and here we showed positive effects of their transplantation on tissue sparing, myelination, angiogenesis, and axonal regeneration compared with the control group, and on myelination, angiogenesis, and axonal regeneration compared with the PNS group. One possible explanation for the functional recovery observed in the SNS group is that the SNS-derived astrocytes provided axonal guidance cues. This idea is supported by previous studies in which glial progenitors or glial progenitor-derived astrocytes were engrafted [28,29,30,31]. Immature astrocytes purified from the postnatal CNS have been shown to promote extensive neurite growth from a variety of neurons [32,33].

Although the reactive astrocytes in glial scar tissue express proteoglycans that can inhibit axonal growth, and have been shown to play a major role in the formation of misaligned scar tissue at sites of injury [34,35,36,37,38], we and others have previously shown that reactive astrocytes also have pivotal roles in the repair of injured tissue and recovery of motor function in the subacute phase after SCI, by sealing off injured areas and preventing the further spread of damage. They also produce an array of neurotrophic and growth factors [39]. Moreover, some astrocytes in the host spinal cord acquire stem-cell properties after injury and hence represent a promising cell type for initiating repair [40]. In combination with host astrocytes, immature astrocytes generated by the grafted SNS may express axonal growth-supporting molecules such as laminin, fibronectin, nerve growth factor (NGF), neurotrophin-3 (NT-3), vasoactive intestinal polypeptide (VIP), and activity-dependent neurotrophic factor (ADNF) [41] with minimal expression of chondroitin sulfate proteoglycans (CSPGs) [42]. In addition, SNS transplantation 9 days after SCI, between the acute and chronic phases, is likely to prevent grafted cells from differentiating into glial scar-forming reactive astrocytes due to their minimal expression of cytokines [3,43] and instead generate immature astrocytes, which provide cues for axonal regeneration. In fact, our immunohistochemical analysis revealed NF-H-positive neuronal fibers aligned with GFAP-positive fibers within the lesion site of the SNS group, suggesting that the SNS transplants promoted the alignment of regenerating axons with the fibers of astrocytes, which in turn promoted axonal growth into and out of the SNS grafts (Fig. 7**A and B**). In addition, the 5-HT-raphespinal system of the spinal cord has been shown to represent axonal regeneration after spinal cord injury [16,17], and the apparent regeneration and/or sparing of host 5-HT-positive fibers elicited by the grafting of SNS may have contributed to the observed functional recovery, since these fibers were not observed in the control or PNS groups (Fig. 6**C and F**).

Another possible explanation for the functional improvement in the SNS group is the enhancement of angiogenesis, since angiogenesis is reported to promote endogenous repair and support axonal outgrowth after SCI [44]. Under hypoxic conditions, astrocytes express angiogenic growth factors, including VEGF [45,46]. We revealed that transplanted SNS, but not PNS, enhanced angiogenesis after SCI (Fig. 5**A–Z**). We observed many host astrocytes (Fig. 5**N–Q**), and a few SNS-graft-derived astrocytes that expressed VEGF (Fig. 5**R–X**), suggesting that the SNS transplants promoted VEGF expression in both the host- and graft-derived GFAP-positive astrocytes. The increase in blood vessels elicited by the transplantation of ES cell-derived gliogenic NS/PCs may have improved axonal growth and prevented atrophy of the injured spinal cord.

The functional improvement might also be due to remyelination by SNS-derived oligodendrocytes, as supported by previous transplantation studies of ES cell-derived NS/PCs or oligodendrocyte progenitor cells (OPCs) [8,47]. While the neurogenic PNS dominantly differentiated into Hu-positive neurons (Fig. 4**F**), the gliogenic SNS differentiated into APC-positive oligodendrocytes that provided MBP-positive sheathes and promoted myelination after SCI (Fig. 2**C, D, F**, and Fig.7**C–F**).

In summary, here we took advantage of our recently established neurosphere-based culture system of ES cell-derived NS/PCs, in which PNS and SNS exhibit neurogenic and gliogenic potentials, respectively, and found that SNS cells were the most effective for promoting recovery after SCI. We showed that grafted SNS generated approximately equal numbers of GFAP-positive astrocytes and APC-positive oligodendrocytes in vivo. Both of these glial cell types may have contributed to the functional recovery, through trophic effects and the promotion of angiogenesis and axonal regeneration by immature astrocytes, and possibly through remyelination by grafted oligodendrocyte progenitor cells. Notably, the transplantation of PNS did not improve the functional recovery after SCI. These findings provide critical information for clinical trials using human ES- and induced pluripotent stem cell (iPS)-derived NS/PC transplantation for SCI.

Moreover, our results suggest that ES cell-derived NS/PCs cultured for relatively long periods may provide sufficient amounts of efficient glial donor cells for cell transplantation therapies. This strategy may also prevent the contamination of tumorigenic undifferentiated ES cells that occurs during long-term culture under serum-free conditions, and support the development of safe embryonic stem cell-based treatment strategies for spinal cord

injury. Although both the CCV-PNS- and CCV-SNS-derived Venus-positive cells survived without forming tumors for 6 weeks after transplantation in this study, careful observation for a longer period will be necessary to assess the possibility of tumor formation.

In the near future, other types of pluripotent stem cells, such as nuclear transfer ES (ntES) and iPS cells, which avoid the risk of immunological rejection and ethical concerns, will need to be evaluated to examine the applicability of human ES cells and human iPS cells in clinical applications.

Materials and Methods

ES Cell Culture and Differentiation

Mouse ES cells (EB3) [13] grown on gelatin-coated (0.1%) tissue-culture dishes were maintained in standard ES cell medium and used for EB formation as previously described, with slight modifications [9,13,48]. For neural induction, ES cells were dissociated into single cells with 0.25% trypsin-EDTA and cultured in bacteriological dishes for 6 days, to allow the formation of EBs. A low concentration of RA (low-RA; 10^{-8} M, Sigma) was added on day 2 of EB formation. The EBs were dissociated into single cells with 0.25% trypsin-EDTA and cultured in suspension at 5×10^4 cells/ml for 7 days in Media hormone mix (MHM) medium with 20 ng/ml FGF2 (Peprotech) and 2% B27 (Invitrogen), to obtain primary neurospheres (PNS). These PNS were dissociated into single cells with TripleLE Select (Invitrogen) and cultured again in suspension at 5×10^4 cells/ml for 7 days under the same conditions, to form secondary neurospheres (SNS) (Fig. 1**B**) [10]. For differentiation analysis, PNS and SNS were allowed to differentiate on poly-L-ornithine/fibronectin-coated coverslips for 5 days, followed by immunocytochemistry. The frequency of colonies consisting of βIII tubulin-positive neurons, GFAP-positive astrocytes, and O4-positive oligodendrocytes (N, A, O: colonies containing more than 20 positive cells are in capital letters; n, a, o: colonies containing fewer than 19 cells are in lower-case letters) is presented as the percentage of total colonies (50 colonies each) from three independent experiments.

Transfection of CAG-CBRluc-IRES-Venus

To visualize transplanted cells by both fluorescence and luminescence, we established an ES cell line that constitutively expresses a click beetle red-emitting luciferase variant (CBR*luc*) [11] and Venus [a yellow fluorescence protein (YFP) mutant] [12] by transfecting a linearized CAG-CBR*luc*-IRES-Venus plasmid (CCV; Fig. 1**A**) into EB3 ES cells using lipofectamine2000 (Invitrogen). Stably transfected ES cells were selected by G418 (200 μg/ml), subcloned, and screened by the expression of both CBR*luc* and Venus. The Venus could be detected by antibodies against EGFP.

Flow Cytometry

Undifferentiated ES cells, PNS, and SNS were dissociated and processed for flow cytometric analysis by FACS Calibur (Becton-Dickinson). The Venus-positive cells were counted and are presented as the percentage of the total number of cells, excluding dead cells stained by propidium iodide.

Spinal Cord Injury Model and Transplantation

Adult female C57BL/6J mice (20–22 g) were anesthetized via intraperitoneal (i.p.) injection of ketamine (100 mg/kg) and xylazine (10 mg/kg). After laminectomy at the 10th thoracic spinal vertebra (T10), a contusive SCI was induced at the same level using a commercially available SCI device (IH impactor, Precision Systems and Instrumentation, Lexington, KY), as described previously [49]. This device creates a reliable contusion injury by rapidly applying a force-defined impact (60 kdyn) with a stainless steel-tipped impounder. The initial touch point of the impactor with the dura was determined (using the vibrator mode of the impactor tip), and from there a 1.5-mm displacement was applied to the spinal cord. Force curve readings revealed an average value of 63±0.5 kdyn.

Nine days after the injury, CCV-PNS (n = 11) or -SNS (n = 11) that had been cultured for 7 days were partially dissociated and transplanted into the lesion epicenter using a glass micropipette (5×10^5 cells/mouse) and stereotaxic injector (KDS 310, Muromachi-kikai, Tokyo, Japan). An equal volume of PBS was injected into the control group (n = 11). Hind limb motor function was evaluated for 6 weeks after SCI using the locomotor rating test of the Basso-Mouse-Scale (BMS), as described previously [21]. Well-trained investigators, blinded to the treatments, performed the behavioral analysis, determining the BMS scores at the same time each day. All animal experiments were approved by the ethics committee of Keio University, and were in accordance with the Guide for the Care and Use of Laboratory Animals (National Institutes of Health, Bethesda, MD).

Bioluminescence Imaging (BLI)

BLI was performed using a Xenogen-IVIS 100 cooled CCD optical macroscopic imaging system (SC BioScience, Tokyo, Japan) [3,50]. To examine the effective expression of CBR*luc in vitro*, we used a CCD-based macroscope detector to determine the luminescence intensity of cultures with various numbers of cells (0 to 5×10^5 cells per well) in the presence of D-luciferin (150 μg/ml). The integration time was fixed at a 5-min duration for each image, and the signals were reported as photons/cells/sec. For *in vivo* BLI, D-luciferin was injected i.p. into mice (150 mg/kg body weight), and serial images were acquired 15–40 min. later, until a maximum signal intensity was obtained with the field-of-view, which was set at 15 cm. We found this time window to be optimal, since the signal intensity peaked 15–40 min after D-luciferin administration, and was followed by a 15-min plateau (data not shown). All images were analyzed with Igor (WaveMetrics, Lake Oswego, OR) and Living Image software (Xenogen, Alameda, CA), and the optical signal intensity was expressed as photon flux, in units of photons/sec/cm^2/steradian. The results were displayed as a pseudocolor photon count image superimposed on a grayscale anatomic image. To quantify the measured light, we defined a region of interest (ROI) over the cell-implanted area and examined all the values within the same ROI. The signal intensity of the engrafted cells was measured weekly for 6 weeks after transplantation.

Histological Analyses

Animals were anesthetized and transcardially perfused with 4% paraformaldehyde in 0.1 M PBS 6 weeks after transplantation. The spinal cords were removed, embedded in OCT compound (Sakura Finetechnical Co., Ltd.), and sectioned in the sagittal/axial plane at 20 μm on a cryostat (Leica CM3050 S). The injured spinal cords from the three groups were histologically evaluated by Hematoxylin-eosin (H-E) staining, Luxol Fast Blue (LFB) staining, and immunohistochemistry. The injured spinal cord from the vehicle control group 2 weeks after SCI was also evaluated by LFB staining and immunohistochemistry for 5-HT. Both cultured cells and tissue sections were stained with the following primary antibodies: anti-GFP (rabbit IgG, 1:500, MBL), anti-βIII tubulin (mouse IgG, 1:1000, Sigma), Alexa488-conjugated anti-βIII tubulin (mouse IgG, 1:4000, Covance), anti-Hu (human IgG,

1:1000, a gift from Dr. Robert Darnell, The Rockefeller University), anti-GFAP (rabbit IgG, 1:4000, Dako), anti-GFAP (guinea pig IgG, 1:4000, Advanced Immunochemical Inc.), anti-GFAP (rat IgG, 1:200, Invitrogen), anti-O4 (mouse IgM, 1:5000, Chemicon), anti-APC CC-1 (mouse IgG, 1:100, Calbiochem), anti-MBP (chicken IgY, 1:200, Aves Labs), anti-Neurofilament RT97 (NF-H, mouse IgG, 1:200, Chemicon), anti-5-HT (goat IgG, 1:200, Immunostar), anti-GAP43 (mouse IgG, 1:2000, Chemicon), Cy3-conjugated anti-SMA (mouse IgG 1:500, Sigma), anti-PECAM-1 (rat IgG, 1:50, BD Bioscience Pharmingen), and anti-VEGF (rabbit IgG, 1:50, Santa Cruz Biotechnology).

For immunohistochemistry with anti-Venus, VEGF, -NF-H, -5-HT, and -GAP43 antibodies, we used a biotinylated secondary antibody (Jackson Immunoresearch Laboratory, Inc.), after exposure to 0.3% H_2O_2 for 30 minutes at room temperature to inactivate endogenous peroxidase. The signals were enhanced with the Vectastain ABC kit (Vector Laboratories, Inc.). Nuclei were stained with Hoechst33258 (10 μg/ml, Sigma). The samples were examined with a universal fluorescence microscope (Axiocam, Carl Zeiss) or a confocal laser scanning microscope (LSM510, Carl Zeiss).

For immunoelectron microscopy, frozen sections were incubated with nanogold-conjugated anti-rabbit secondary antibody (1:100 Invitrogen) followed by incubation with the primary anti-GFP antibody. After enhancement with HQ-Silver kit (Nanoprobes Inc.), sections were postfixed with 0.5% osmium tetroxide, dehydrated through ethanol, and embedded in Epon. Ultrathin sections were stained with uranyl acetate and lead citrate, observed under a transmission EM (JEOL model 1230), and photographed with a Digital Micrograph 3.3 (Gatan Inc.).

Quantitative Analyses of Stained Tissue Sections through Transplanted Spinal Cord

To quantify HE-, LFB-, or immunostained sections, images were obtained by a universal fluorescence microscope (Axiocam, Carl Zeiss), manually outlined, and quantified by Micro Computer Imaging Device (MCID; Imaging Research Inc., St. Catharines, Ontario, Canada). Constant threshold values were maintained for all the analyses with MCID. HE-stained images were taken at the lesion epicenter and 2, 1, and 0.5 mm rostral and caudal to the epicenter in axial sections at ×25 magnification (n = 5, each). To analyze the LFB-positive area after transplantation, we automatically captured four regions from each animal in axial sections at the lesion epicenter and 2 mm and 1 mm rostral and caudal to the epicenter at ×200 magnification. Analyses were performed 2 weeks or 6 weeks after SCI for the vehicle-control group and 6 weeks after for the PNS and SNS groups. The total myelinated area was quantified by MCID using light intensity gain counting (n = 3, each). For the Venus (GFP)-positive area after transplantation, we captured in midsagittal sections the epicenter at ×25 magnification from each animal (6 weeks after SCI for the vehicle-control, PNS, and SNS groups), and quantified the total Venus-positive area (n = 6, each). NF-H-stained images were taken at the epicenter and 4, 3, 2, 1, and 0.5 mm rostral and caudal to the epicenter in axial sections at ×50 magnification, and the NF-H-positive areas were quantified using light intensity gain counting (n = 5, each). VEGF-stained images were taken at the lesion epicenter in axial sections at ×50, and the VEGF-positive areas were quantified using light intensity gain counting (n = 3, each). To analyze the 5-HT-positive area after transplantation, we automatically captured five regions from each animal in axial sections 4-mm caudal to the lesion epicenter (Th10 level), which was approximately at the L1 level, a non-lesion site, at ×200 magnification. The analysis was performed 2 weeks or 6 weeks after SCI for the vehicle-control group and 6 weeks after for the PNS and SNS groups. The total 5-HT-positive area was quantified (n = 3, for each condition). For the GAP43-positive area after transplantation, we captured the ventral regions in midsagittal sections 1 mm caudal to the epicenter at ×200 magnification from each animal (6 weeks after SCI for the vehicle-control, PNS, and SNS groups), and quantified the total GAP43-positive area (n = 4). To quantify the proportion of cells positive for each cell type-specific marker *in vivo*, we selected representative midsagittal sections and automatically captured five regions within 500 μm rostral and caudal to the lesion epicenter at ×200. The engrafted cells in each section that were positive for both Venus and each cell type-specific marker were counted (n = 4). The PECAM-1-positive blood vessels were counted manually in axial sections of the lesion epicenter at ×200 magnification (n = 3, each).

Statistical Analysis

All data are presented as the mean ± s.e.m. An unpaired two-tailed Student's *t*-test was used for the BLI analyses and Venus-stained analysis, and *in vivo* differentiation assays. ANOVA followed by the Turkey-Kramer test for multiple comparisons among the three transplantation groups was used for the *in vivo* differentiation analysis and PECAM-1-, VEGF-, 5HT-, and GAP43-stained analysis. Repeated measures two-way ANOVA followed by the Turkey-Kramer test was used for HE-, LFB-, NF-H-stained and BMS analysis. Pearson's correlation coefficient was used for correlation of the results of BLI analysis and the quantification of Venus-positive area. In all statistical analyses, the significance was set at $P<0.05$.

Acknowledgments

We thank Drs. H. J. Okano, K. Ishii, W. Akamatsu, S. Ishii, K. Miura, T. Nagai, S. Miyao, and T. Harada for technical assistance and scientific discussion, and all the members of Dr. Okano's laboratory for encouragement and kind support. We thank Drs. Y. Ishibashi, E. Tsuda, T. Yokoyama, and A. Ono for encouragement and kind support. We also thank Dr. H. Niwa for the EB3 cells.

Author Contributions

Conceived and designed the experiments: GK YO YT MN HO. Performed the experiments: GK YO JY NN KK MM OT KF HK SS. Analyzed the data: GK MN. Contributed reagents/materials/analysis tools: GK YO SO SS YM ST MN HO. Wrote the paper: GK YO HK MN HO.

References

1. Ogawa Y, Sawamoto K, Miyata T, Miyao S, Watanabe M, et al. (2002) Transplantation of in vitro-expanded fetal neural progenitor cells results in neurogenesis and functional recovery after spinal cord contusion injury in adult rats. J Neurosci Res 69: 925–933.
2. Iwanami A, Kaneko S, Nakamura M, Kanemura Y, Mori H, et al. (2005) Transplantation of human neural stem cells for spinal cord injury in primates. J Neurosci Res 80: 182–190.
3. Okada S, Ishii K, Yamane J, Iwanami A, Ikegami T, et al. (2005) In vivo imaging of engrafted neural stem cells: its application in evaluating the optimal timing of transplantation for spinal cord injury. Faseb J 19: 1839–1841.
4. Hofstetter CP, Holmstrom NA, Lilja JA, Schweinhardt P, Hao J, et al. (2005) Allodynia limits the usefulness of intraspinal neural stem cell grafts; directed differentiation improves outcome. Nat Neurosci 8: 346–353.
5. Cummings BJ, Uchida N, Tamaki SJ, Salazar DL, Hooshmand M, et al. (2005) Human neural stem cells differentiate and promote locomotor recovery in spinal cord-injured mice. Proc Natl Acad Sci U S A 102: 14069–14074.
6. Bibel M, Richter J, Schrenk K, Tucker KL, Staiger V, et al. (2004) Differentiation of mouse embryonic stem cells into a defined neuronal lineage. Nat Neurosci 7: 1003–1009.

7. McDonald JW, Liu XZ, Qu Y, Liu S, Mickey SK, et al. (1999) Transplanted embryonic stem cells survive, differentiate and promote recovery in injured rat spinal cord. Nat Med 5: 1410–1412.
8. Keirstead HS, Nistor G, Bernal G, Totoiu M, Cloutier F, et al. (2005) Human embryonic stem cell-derived oligodendrocyte progenitor cell transplants remyelinate and restore locomotion after spinal cord injury. J Neurosci 25: 4694–4705.
9. Okada Y, Shimazaki T, Sobue G, Okano H (2004) Retinoic-acid-concentration-dependent acquisition of neural cell identity during in vitro differentiation of mouse embryonic stem cells. Dev Biol 275: 124–142.
10. Okada Y, Matsumoto A, Shimazaki T, Enoki R, Koizumi A, et al. (2008) Spatio-Temporal Recapitulation of Central Nervous System Development By Murine ES Cell-Derived Neural Stem/Progenitor Cells. Stem Cells.
11. Zhao H, Doyle TC, Coquoz O, Kalish F, Rice BW, et al. (2005) Emission spectra of bioluminescent reporters and interaction with mammalian tissue determine the sensitivity of detection in vivo. J Biomed Opt 10: 41210.
12. Nagai T, Ibata K, Park ES, Kubota M, Mikoshiba K, et al. (2002) A variant of yellow fluorescent protein with fast and efficient maturation for cell-biological applications. Nat Biotechnol 20: 87–90.
13. Niwa H, Miyazaki J, Smith AG (2000) Quantitative expression of Oct-3/4 defines differentiation, dedifferentiation or self-renewal of ES cells. Nat Genet 24: 372–376.
14. Wang X, Rosol M, Ge S, Peterson D, McNamara G, et al. (2003) Dynamic tracking of human hematopoietic stem cell engraftment using in vivo bioluminescence imaging. Blood 102: 3478–3482.
15. Contag CH, Bachmann MH (2002) Advances in in vivo bioluminescence imaging of gene expression. Annu Rev Biomed Eng 4: 235–260.
16. Bregman BS (1987) Spinal cord transplants permit the growth of serotonergic axons across the site of neonatal spinal cord transection. Brain Res 431: 265–279.
17. Saruhashi Y, Young W, Perkins R (1996) The recovery of 5-HT immunoreactivity in lumbosacral spinal cord and locomotor function after thoracic hemisection. Exp Neurol 139: 203–213.
18. Ramon-Cueto A, Plant GW, Avila J, Bunge MB (1998) Long-distance axonal regeneration in the transected adult rat spinal cord is promoted by olfactory ensheathing glia transplants. J Neurosci 18: 3803–3815.
19. Kaneko S, Iwanami A, Nakamura M, Kishino A, Kikuchi K, et al. (2006) A selective Sema3A inhibitor enhances regenerative responses and functional recovery of the injured spinal cord. Nat Med 12: 1380–1389.
20. Kobayashi NR, Fan DP, Giehl KM, Bedard AM, Wiegand SJ, et al. (1997) BDNF and NT-4/5 prevent atrophy of rat rubrospinal neurons after cervical axotomy, stimulate GAP-43 and Talpha1-tubulin mRNA expression, and promote axonal regeneration. J Neurosci 17: 9583–9595.
21. Basso DM, Fisher LC, Anderson AJ, Jakeman LB, McTigue DM, et al. (2006) Basso Mouse Scale for locomotion detects differences in recovery after spinal cord injury in five common mouse strains. J Neurotrauma 23: 635–659.
22. Coutts M, Keirstead HS (2007) Stem cells for the treatment of spinal cord injury. Exp Neurol.
23. Temple S (2001) The development of neural stem cells. Nature 414: 112–117.
24. Fan G, Martinowich K, Chin MH, He F, Fouse SD, et al. (2005) DNA methylation controls the timing of astrogliogenesis through regulation of JAK-STAT signaling. Development 132: 3345–3356.
25. Shimozaki K, Namihira M, Nakashima K, Taga T (2005) Stage- and site-specific DNA demethylation during neural cell development from embryonic stem cells. J Neurochem 93: 432–439.
26. Takizawa T, Nakashima K, Namihira M, Ochiai W, Uemura A, et al. (2001) DNA methylation is a critical cell-intrinsic determinant of astrocyte differentiation in the fetal brain. Dev Cell 1: 749–758.
27. Winkler C, Fricker RA, Gates MA, Olsson M, Hammang JP, et al. (1998) Incorporation and glial differentiation of mouse EGF-responsive neural progenitor cells after transplantation into the embryonic rat brain. Mol Cell Neurosci 11: 99–116.
28. Hofstetter CP, Schwarz EJ, Hess D, Widenfalk J, El Manira A, et al. (2002) Marrow stromal cells form guiding strands in the injured spinal cord and promote recovery. Proc Natl Acad Sci U S A 99: 2199–2204.
29. Hill CE, Proschel C, Noble M, Mayer-Proschel M, Gensel JC, et al. (2004) Acute transplantation of glial-restricted precursor cells into spinal cord contusion injuries: survival, differentiation, and effects on lesion environment and axonal regeneration. Exp Neurol 190: 289–310.
30. Cao Q, Xu XM, Devries WH, Enzmann GU, Ping P, et al. (2005) Functional recovery in traumatic spinal cord injury after transplantation of multineurotrophin-expressing glial-restricted precursor cells. J Neurosci 25: 6947–6957.
31. Davies JE, Huang C, Proschel C, Noble M, Mayer-Proschel M, et al. (2006) Astrocytes derived from glial-restricted precursors promote spinal cord repair. J Biol 5: 7.
32. Baehr M, Bunge RP (1990) Growth of adult rat retinal ganglion cell neurites on astrocytes. Glia 3: 293–300.
33. Noble M, Fok-Seang J, Cohen J (1984) Glia are a unique substrate for the in vitro growth of central nervous system neurons. J Neurosci 4: 1892–1903.
34. Tang X, Davies JE, Davies SJ (2003) Changes in distribution, cell associations, and protein expression levels of NG2, neurocan, phosphacan, brevican, versican V2, and tenascin-C during acute to chronic maturation of spinal cord scar tissue. J Neurosci Res 71: 427–444.
35. Bundesen LQ, Scheel TA, Bregman BS, Kromer LF (2003) Ephrin-B2 and EphB2 regulation of astrocyte-meningeal fibroblast interactions in response to spinal cord lesions in adult rats. J Neurosci 23: 7789–7800.
36. De Winter F, Oudega M, Lankhorst AJ, Hamers FP, Blits B, et al. (2002) Injury-induced class 3 semaphorin expression in the rat spinal cord. Exp Neurol 175: 61–75.
37. Moreau-Fauvarque C, Kumanogoh A, Camand E, Jaillard C, Barbin G, et al. (2003) The transmembrane semaphorin Sema4D/CD100, an inhibitor of axonal growth, is expressed on oligodendrocytes and upregulated after CNS lesion. J Neurosci 23: 9229–9239.
38. Berry M, Maxwell WL, Logan A, Mathewson A, McConnell P, et al. (1983) Deposition of scar tissue in the central nervous system. Acta Neurochir Suppl (Wien) 32: 31–53.
39. Okada S, Nakamura M, Katoh H, Miyao T, Shimazaki T, et al. (2006) Conditional ablation of Stat3 or Socs3 discloses a dual role for reactive astrocytes after spinal cord injury. Nat Med 12: 829–834.
40. Buffo A, Rite I, Tripathi P, Lepier A, Colak D, et al. (2008) Origin and progeny of reactive gliosis: A source of multipotent cells in the injured brain. Proc Natl Acad Sci U S A 105: 3581–3586.
41. Blondel O, Collin C, McCarran WJ, Zhu S, Zamostiano R, et al. (2000) A glia-derived signal regulating neuronal differentiation. J Neurosci 20: 8012–8020.
42. Gallo V, Bertolotto A (1990) Extracellular matrix of cultured glial cells: selective expression of chondroitin 4-sulfate by type-2 astrocytes and their progenitors. Exp Cell Res 187: 211–223.
43. Nakamura M, Houghtling RA, MacArthur L, Bayer BM, Bregman BS (2003) Differences in cytokine gene expression profile between acute and secondary injury in adult rat spinal cord. Exp Neurol 184: 313–325.
44. Beattie MS, Bresnahan JC, Komon J, Tovar CA, Van Meter M, et al. (1997) Endogenous repair after spinal cord contusion injuries in the rat. Exp Neurol 148: 453–463.
45. Mense SM, Sengupta A, Zhou M, Lan C, Bentsman G, et al. (2006) Gene expression profiling reveals the profound upregulation of hypoxia-responsive genes in primary human astrocytes. Physiol Genomics 25: 435–449.
46. Yoshida H, Imaizumi T, Tanji K, Matsumiya T, Sakaki H, et al. (2002) Platelet-activating factor enhances the expression of vascular endothelial growth factor in normal human astrocytes. Brain Res 944: 65–72.
47. Liu S, Qu Y, Stewart TJ, Howard MJ, Chakrabortty S, et al. (2000) Embryonic stem cells differentiate into oligodendrocytes and myelinate in culture and after spinal cord transplantation. Proc Natl Acad Sci U S A 97: 6126–6131.
48. Hooper M, Hardy K, Handyside A, Hunter S, Monk M (1987) HPRT-deficient (Lesch-Nyhan) mouse embryos derived from germline colonization by cultured cells. Nature 326: 292–295.
49. Scheff SW, Rabchevsky AG, Fugaccia I, Main JA, Lumpp JE, Jr. (2003) Experimental modeling of spinal cord injury: characterization of a force-defined injury device. J Neurotrauma 20: 179–193.
50. Rice BW, Cable MD, Nelson MB (2001) In vivo imaging of light-emitting probes. J Biomed Opt 6: 432–440.

Journal of Neuroscience Research

Journal of Neuroscience Research 88:1394–1405 (2010)

Transplantation of Galectin-1-Expressing Human Neural Stem Cells Into the Injured Spinal Cord of Adult Common Marmosets

Junichi Yamane,[1,2] Masaya Nakamura,[2] Akio Iwanami,[1,2,3] Masanori Sakaguchi,[1] Hiroyuki Katoh,[2,3] Masayuki Yamada,[4,5] Suketaka Momoshima,[6] Sachiyo Miyao,[1,2] Ken Ishii,[2] Norikazu Tamaoki,[4] Tatsuji Nomura,[4] Hirotaka James Okano,[1] Yonehiro Kanemura,[7] Yoshiaki Toyama,[2] and Hideyuki Okano[1]*

[1]Department of Physiology, Keio University School of Medicine, Shinjuku, Tokyo, Japan
[2]Department of Orthopedic Surgery, Keio University School of Medicine, Shinjuku, Tokyo, Japan
[3]Research Division, National Organization, Murayama Medical Center, Tokyo, Japan
[4]Central Institute for Experimental Animals, Kawasaki, Kanagawa, Japan
[5]Faculty of Radiological Technology, Fujita Health University School of Health Sciences, Aichi, Japan
[6]Department of Radiology, Keio University School of Medicine, Shinjuku, Tokyo, Japan
[7]Institute for Clinical Research, Osaka National Hospital, National Hospital Organization, Osaka, Japan

Delayed transplantation of neural stem/progenitor cells (NS/PCs) into the injured spinal cord can promote functional recovery in adult rats and monkeys. To enhance the functional recovery after NS/PC transplantation, we focused on galectin-1, a carbohydrate-binding protein with pleiotropic roles in cell growth, differentiation, apoptosis, and neurite outgrowth. Here, to determine the combined therapeutic effect of NS/PC transplantation and galectin-1 on spinal cord injury (SCI), human NS/PCs were transfected by lentivirus with galectin-1 and green fluorescent protein (GFP), (Gal-NS/PCs) or GFP alone (GFP-NS/PCs), expanded in vitro, and then transplanted into the spinal cord of adult common marmosets, 9 days after contusive cervical SCI. The animals' motor function was evaluated by their spontaneous motor activity, bar grip power, and performance on a treadmill test. Histological analyses revealed that the grafted human NS/PCs survived and differentiated into neurons, astrocytes, and oligodendrocytes. There were significant differences in the myelinated area, corticospinal fibers, and serotonergic fibers among the Gal-NS/PC, GFP-NS/PC, vehicle-control, and sham-operated groups. The Gal-NS/PC-grafted animals showed a better performance on all the behavioral tests compared with the other groups. These findings suggest that Gal-NS/PCs have better therapeutic potential than NS/PCs for SCI in nonhuman primates and that human Gal-NS/PC transplantation might be a feasible treatment for human SCI.

Key words: spinal cord injury; galectin-1; common marmoset; neural stem/progenitor cells; preclinical study

It has long been believed that the adult mammalian central nervous system (CNS) does not regenerate after injury. In particular, spinal cord injury (SCI) has been intractable to neural regeneration and functional recovery (Horner and Gage, 2000; Okano, 2002a,b), owing to, among other factors, the limited ability of the CNS to replace lost cells (Johansson et al., 1999), axonal growth inhibitors associated with CNS myelin, fibrous and glial scars (Olson, 2002; David and Lacroix, 2003), and insufficient trophic support (Widenfalk et al., 2001). With recent progress in stem cell biology, however, several types of cells have become potential transplantation candidates for treating SCI, including embryonic stem (ES) cell-derived cells (McDonald et al., 1999; Keirstead et al., 2005), mesenchymal stem cells (MSCs; Hofstetter et al., 2002), olfactory ensheathing cells (OECs; Li et al., 1997), nestin-expressing multipotent hair follicle stem cells (Li et al., 2003; Amoh et al., 2008), and neural

Contract grant sponsor: Project to Realize Regenerative Medicine from the Japanese Ministry of Education, Sports and Culture; Human Frontier Science Program Organization; Contract grant sponsor: Core Research for Evolutional Science and Technology (CREST) from the Japan Science and Technology Corporation (JST); Contract grant sponsor: General Insurance Association of Japan; Contract grant sponsor: National Grant-in-Aid for the Establishment of a High-Tech Research Center in a Private University in Japan; Contract grant sponsor: Keio University Special Grant-in-Aid for Innovative Collaborative Research Projects (to H.O.); Contract grant sponsor: Grant-in-Aid from the Global COE Program of the Ministry of Education, Culture, Sports, Science and Technology, Japan (to Keio University); Contract grant sponsor: Keio University Grant-in-Aid for the Encouragement of Young Medical Scientists (to J.Y.).

*Correspondence to: Hideyuki Okano, Department of Physiology, Keio University School of Medicine, 35 Shinanomachi, Shinjuku, Tokyo, 160-8582, Japan. E-mail: hidokano@sc.itc.keio.ac.jp

Received 8 August 2009; Revised 3 October 2009; Accepted 19 October 2009

Published online 20 January 2010 in Wiley InterScience (www.interscience.wiley.com). DOI: 10.1002/jnr.22322

stem cells (NS/PCs; Cao et al., 2001; Ogawa et al., 2002).

To establish therapies involving NS/PC transplantation for SCI, we previously reported that the transplantation of rat NS/PCs promotes functional recovery after SCI in neonatal (Nakamura et al., 2005) and adult rats (Ogawa et al., 2002). We also established a graded SCI model in common marmosets (Iwanami et al., 2005b) and found that transplanted human NS/PCs promoted functional recovery after the injury in this model (Iwanami et al., 2005a). However, the observed functional recovery after NS/PC transplantation was not sufficient to qualify the procedure for a clinical trial in patients with complete SCI. Therefore, we have been seeking ways to enhance the functional recovery following NS/PC transplantation.

Lectins are carbohydrate-binding proteins with an affinity for β-galactoside-containing glycol conjugates. Galectin-1 (Gal-1) is a lectin observed in various normal and pathological tissues that appears to be functionally pleiotropic, with roles in a wide range of biological processes, including cell growth and differentiation, apoptosis, cell adhesion, tumor spreading, neurite outgrowth, and inflammation (Outenreath and Jones, 1992; Mahanthappa et al., 1994; Perillo et al., 1995, 1998; Puche et al., 1996; Rabinovich et al., 2000a,b, 2002). Previous reports demonstrated that Gal-1 is expressed on adult NS/PCs and promotes their proliferation through its carbohydrate-binding activity in the CNS (Sakaguchi et al., 2006). Furthermore, Gal-1 administration exhibited therapeutic effects against focal brain ischemia (Ishibashi et al., 2007) and also enhanced peripheral axonal regeneration (Horie et al., 1999). The purpose of the present study was to determine the effectiveness of transplanting human galectin-1-expressing human NS/PCs in promoting the recovery of motor functions in tetraplegic primates after contusive SCI.

MATERIALS AND METHODS

Tissue Samples and Neural Stem Cell Cultures

The ethical committees of Osaka National Hospital, the Tissue Engineering Research Center, and Keio University approved the use of human fetal neural tissues and neurosphere cultures. Tissue procurement was in accordance with the Declaration of Helsinki and in agreement with the ethical guidelines of the Network of European CNS Transplantation and Restoration (NECTAR) and the Japan Society of Obstetrics and Gynecology. Written informed consent was obtained from all the parents. By using the neurosphere culture method (Reynolds and Weiss, 1996; Nakamura et al., 2003), neural stem cells (NS/PCs) were cultured from the forebrain tissue of human fetuses (10 weeks gestational age) that were obtained through routine legal terminations performed at Osaka National Hospital.

Lentiviral Vector Expressing the h-Galectin-1 Gene

The third-generation self-inactivating HIV-1-based lentiviral vector, pCSII-EF-MCS-IRES2-Venus (Miyoshi et al., 1998), contained an internal ribosomal entry site (IRES); Venus, a variant of GFP (Nagai et al., 2002); and a woodchuck hepatitis virus post-transcriptional regulatory element (PRE). The h-galectin-1 gene fragment was excised from a human cDNA library and cloned into pCSII-EF-MCS-IRES2-Venus at the BamH1 site (Fig. 1A). Twenty-four hours before transfection, 293T cells were seeded in poly-L-lysine-coated T175 flasks. The cells were transfected using the lipofection protocol for the FuGENE6 transfection reagent (Roche, Indianapolis, IN). Two days after transfection, the conditioned medium was collected, and the virus was concentrated by centrifugation at 79,000*g* for 2 hr at 4°C. The pelleted virus was resuspended and stored at −80°C. The titer of the concentrated virus was approximately 5×10^8 transducing units per milliliter (TU/ml) when assayed using 293T cells, and infectivity was determined by the expression of GFP, which was analyzed by using a FACSCalibur (Becton-Dickinson, Franklin Lakes, NJ).

Lentiviral Transduction of Human NS/PCs

Human NS/PCs (hNS/PCs) that had undergone more than 10 passages by the neurosphere method were dissociated into single cells 2 hr before being infected. The concentrated viruses were then added to the culture medium to infect the hNS/PCs [multiplicity of infection (MOI) = 1.0]. Two weeks later, neurospheres were formed from the dissociated hNS/PCs (Fig. 1B) and were passaged as previously reported (Reynolds and Weiss, 1996; Nakamura et al., 2003). The efficiency of the transduction was measured by GFP expression with a FACSCalibur, as in the analysis of viral infectivity, and hNS/PCs with an efficiency of transduction greater than 80% were used for transplantation. Two types of lentivirus-transduced hNS/PCs were prepared: Gal-NS/PCs, hNS/PCs infected with the h-galectin-1 IRES Venus virus; and GFP-NS/PCs, hNS/PCs infected with the IRES Venus virus. Gal-NS/PCs, GFP-NS/PCs, and vehicle only were transplanted into the injured spinal cord. The expression of h-galectin-1 in all the hNS/PCs (Gal-NS/PCs, GFP-NS/PCs, and naive NS/PCs) was examined by Western blotting of cell lysates and conditioned media.

Proliferation Assay

The number of viable cells was indirectly analyzed by measuring ATP, a product of cell metabolism. After incubating the cultures in microplates at 37°C in 5% CO_2, 95% air for 24 hr or 144 hr, an ATP assay (CellTiter-GloTM Luminescent Cell Viability Assay; Promega, Madison, WI) was carried out according to the manufacturer's instructions. Briefly, 100 μl of Cell Titer-GloTM Reagent was added to each well, and the plate was incubated for 30 min at room temperature. The luminescent signal was detected using a chemiluminescence detection system (Wallac 1420 ARVOSX; Perkin-Elmer). The population doubling time (DT) was determined by using the ATP assay as described elsewhere (Kanemura et al., 2002).

Differentiation Assay

After the second passage, neurospheres prepared from Gal-NS/PCs, GFP-NS/PCs, or naive NS/PCs were dissociated into single cells and plated onto poly-L-lysine-coated

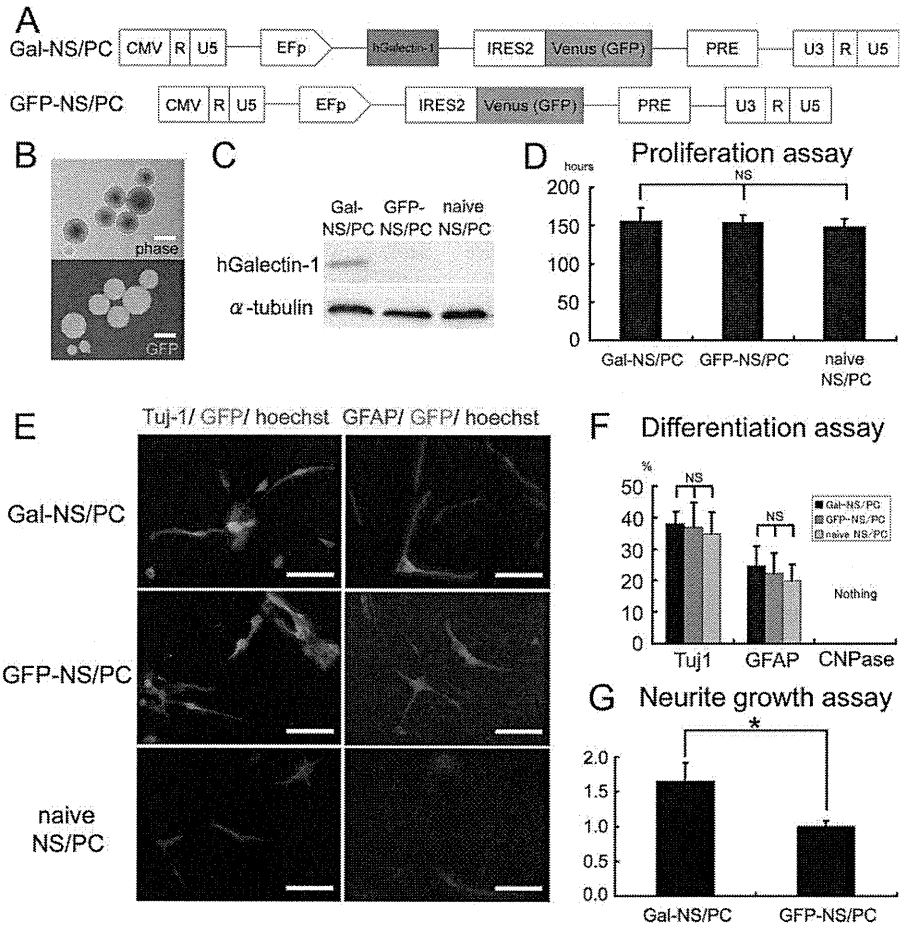

Fig. 1. Characterization of human NS/PCs in vitro. **A**: Lentiviral construct encoding a dual-function h-galectin-1 and GFP bicistronic reporter gene connected via an internal ribosomal entry site (IRES). **B**: Microscopic images of the lentivirally transduced human NS/PCs. **C**: Western blotting for h-galectin-1. A higher level of h-galectin-1 expression was observed in the Gal-NS/PCs. **D**: ATP assay. There was no significant difference in the proliferation rate among Gal-NS/PCs, GFP-NS/PCs, and naive NS/PCs. **E**: Differentiation assay. Lentiviral transfection did not influence the phenotype of human NS/PCs. Immunocytochemistry revealed that all of the human NS/PCs differentiated into Tuj1$^+$ neurons and GFAP$^+$ astrocytes, but not CNPase$^+$ oligodendrocytes (not shown), in vitro. **F**: Quantitative analyses of the differentiated phenotype of human NS/PCs. The proportions of the differentiated phenotypes in the lentivirally transduced NS/PCs (Gal-NS/PCs and GFP-NS/PCs) were identical to those of the untreated naive NS/PCs. **G**: Neurite growth assay. The neurites were significantly longer in the neurons derived from Gal-NS/PCs than in those derived from GFP-NS/PCs. The average length in GFP-NS/PCs was defined as 1.0. $*P < 0.05$. Scale bars = 100 μm in B; 50 μm in E.

coverslips at a density of 1×10^5 cells/ml in 10% FCS-containing medium. After 7 days in culture, the cells were fixed with 4% paraformaldehyde (PFA) in 0.1 M phosphate-buffered saline (PBS) for immunocytochemistry. Cultured cells were immunostained with the following primary antibodies: anti-GFP (1:500; MBL, Woburn, MA), anti-glial fibrillary acid protein (GFAP; 1:1,000; Dako, Glostrup, Denmark), anti-βIII tubulin (Tuj-1; 1:200; Sigma, St. Louis, MO), and anti-2′,3′-cyclic nucleotide 3′-phosphodiesterase (CNPase; 1:200; Sigma). Nuclei were counterstained with Hoechst 33342 (Molecular Probes, Eugene, OR). All images were obtained with a fluorescence microscope (Axioskop 2 plus; Carl Zeiss, Munich, Germany). After the differentiation assay, the neurite length of hNS/PCs that were double positive for GFP and βIII tubulin was measured by the MCID (microcomputer imaging device) system (Amersham Bioscience Corp., Piscataway, NJ). The neurite length of the Gal-NS/PCs relative to that of GFP-NS/PCs was determined.

Contusive SCI in Common Marmosets

Adult female common marmosets (*Callithrix jacchus*; Clea Japan Inc., Tokyo, Japan) were anesthetized with intramuscular injections of ketamine (50 mg/kg; Sankyo Co., Ltd., Tokyo, Japan) and xylazine (5 mg/kg; Bayer AG, Leverkusen, Germany) and by the inhalation of isofluren (Foren; Abbott Japan Co., Ltd., Tokyo, Japan). A moderate contusive SCI was induced in 21 marmosets using a modified NYU device, as previously reported (Iwanami et al., 2005b). In brief, a 17-g weight (3.5-mm in diameter) was dropped from a height of 50 mm onto the exposed dura mater at the C5 level. In the laminectomy group (n = 2), only a laminectomy was per-

formed. All the animals were placed in a temperature-controlled chamber until thermoregulation was reestablished. Micturition by manual bladder compression was performed twice per day until voiding reflexes were reestablished. Paralyzed animals were fed manually until they recovered their ability to ingest food and water without assistance. For 1 week after surgery, ampicillin (100 mg/kg; Meiji Seika Kaisha, Ltd., Tokyo, Japan) was injected intramuscularly into each animal. Prior approval of all animal procedures, which were in accordance with the NIH *Guide for the care and use of laboratory animals,* was obtained from the Keio University Ethics Committee and the Animal Experimentation Committee of the Central Institute for Experimental Animals.

Transplantation of hNS/PCs

hNS/PCs were transplanted into the injured spinal cord 9 days after the injury, at which time the microenvironment of the injured spinal cord changes from the inhospitable setting of the acute phase to one that supports the survival and differentiation of transplanted NS/PCs (Ogawa et al., 2002; Okano, 2002a; Nakamura et al., 2003; Okano et al., 2003). After the animals were again anesthetized, partially dissociated neurospheres at a density of approximately 1.0×10^6 cells/5 μl in medium without growth factors (Gal-NS/PCs or GFP-NS/PCs, n = 7) or a medium vehicle without growth factors (vehicle-control group, n = 7) were injected into the lesion epicenter using a glass pipette fitted to a 25-μl Hamilton syringe and a microstereotaxic injection system (David Kopf Instruments, Tujunga, CA). All the animals received daily ampicillin for 1 week after the transplantation and daily subcutaneous cyclosporine injections (10 mg/kg; Novartis, Basel, Switzerland) until they were sacrificed for analysis.

MRI

The magnitude of the SCI and the changes after injury were evaluated by magnetic resonance imaging (MRI), with which pathogenic events such as hemorrhage, edema, and cavity formation can be assessed in real time (Ohta et al., 1999; Metz et al., 2000). With a 7.0-Tesla superconducting imager (Bruker, Rheinstetten, Germany) fitted with a phased-array volume coil, MRI of the injured spinal cord was conducted 3 days after injury and 12 weeks after transplantation under the following conditions: 1) sagittal and 2) axial T2-weighted (T2W) fast spin-echo with a TR/TE number averaging 4,000 msec/100 msec/15, field-of-view of 9 cm, matrix of 256 × 256, and section thickness of 1.7 mm, and 3) sagittal T1-weighted (T1W) spin echo with a TR/TE number averaging 400 msec/12 msec/15 (all other parameters the same as given above).

Behavioral Analyses

The motor function of all the common marmosets was evaluated by measuring their spontaneous motor activity and bar grip power, as previously described (Iwanami et al., 2005b) and by introducing a treadmill test to assess higher locomotor function.

Measurement of spontaneous motor activity. Spontaneous motor activity is difficult to evaluate in common marmosets because of their three-dimensional movement (that is, they climb as well as walk around their enclosures). In the present study, we used cages (350-mm wide, 500-mm deep, 500-mm high) equipped with infrared sensors (Murata Manufacturing Corp., Nagaokakyo, Kyoto, Japan) on the ceiling and continually recorded the marmosets' motions in all three dimensions. The data were uploaded to a computer every hour, and the activity after SCI was quantified and expressed as a percentage of the animal's activity before the injury (Iwanami et al., 2005b).

Bar grip power. The motor function of the upper extremities was evaluated by a bar grip power test, which examines the animal's gripping reflex (the motion undertaken when attempting to grasp an object placed before the animal). The test was performed three times per day, and the maximal grip strength as a percentage of that before the injury was calculated (Iwanami et al., 2005b).

Treadmill test. The locomotive function of each marmoset was evaluated by using a treadmill test. The maximum velocity at which the animal could walk or run was recorded once per week, and the velocity after SCI as a percentage of that before the injury was calculated.

Histological Analyses

Thirteen weeks after transplantation, each animal was deeply anesthetized and intracardially perfused with 4% PFA (pH 7.4). The spinal cord tissues were removed, postfixed in 4% PFA, and immersed overnight in 10% sucrose followed by 30% sucrose. The cord was then embedded in OCT compound and sectioned on a cryostat at 20 μm for axial sections and 30 μm for sagittal sections. The sections were stained with hematoxylin-eosin (H-E) for general histological examinations and with Luxol fast blue (LFB) to evaluate the myelinated area after SCI. The area of myelinated fibers in axial sections of the lesion epicenter was measured using the MCID system and compared among the three (Gal-NS/PC, GFP-NS/PC, or vehicle-control) groups. To assess the corticospinal tract (CST), sections were immunostained with an anticalmodulin-dependent protein kinase II alpha (CaMKIIα) antibody (1:100; mouse monoclonal; Zymed, CA; secondary antibody was HRP-labeled goat anti-mouse IgG for TSA, ABC, and DAB staining), and the serotonergic fibers were immunostained with an anti-5HT antibody (1:100; rabbit polyclonal; Diasorin, Venice, Italy; secondary antibody was Alexa 568 goat anti-rabbit IgG; 1:500; Molecular Probes). The total areas positive for CaMKIIα or 5HT in axial sections of the lesion epicenter were measured using the MCID system and compared among the three groups.

The hNS/PCs grafted into the injured spinal cords were identified by using an anti-GFP antibody (1:200; MBL), and their phenotypes were examined by immunostaining for the following cell-type-specific markers: antiglutathione S-transferase pi (GSTpi; 1:500; mouse monoclonal; BD Biosciences, San Jose, CA), anti-Hu (Okano and Darnell, 1997; 1:200; a gift from R. Darnell, The Rockefeller University), and anti-GFAP (1:200; Dako, Glostrup, Denmark). To evaluate associations between the grafted cells and the host axons or myelin sheath around the lesion epicenter, triple immunostaining for

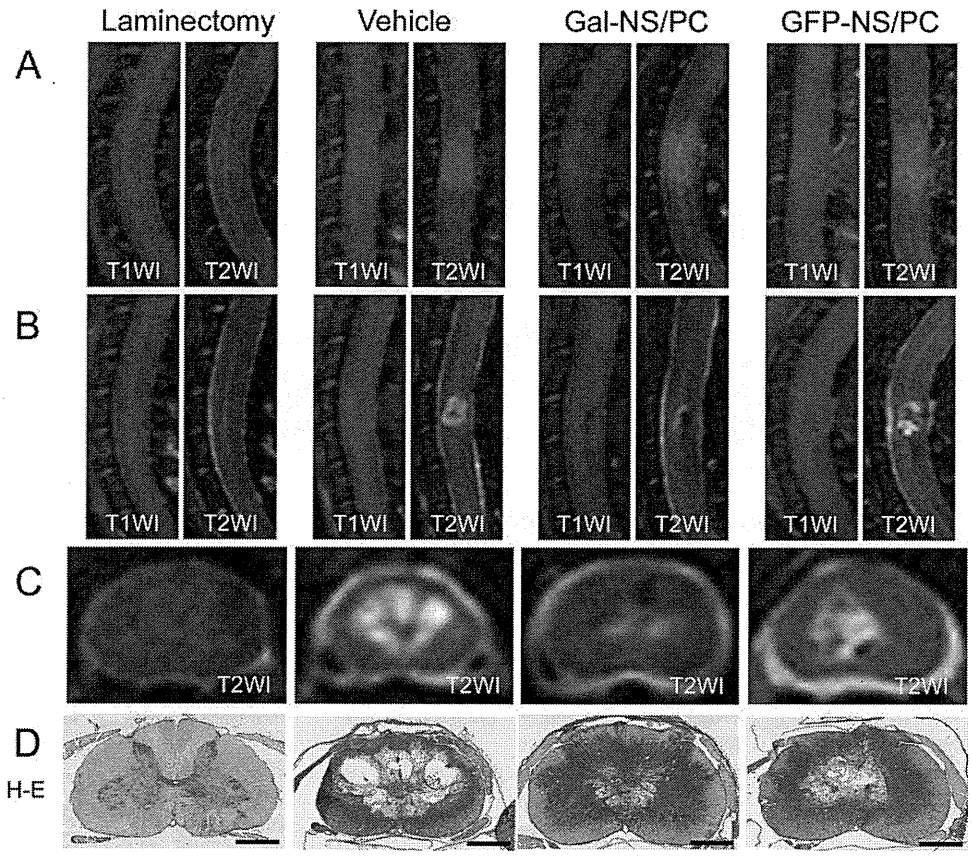

Fig. 2. Comparisons of the injured spinal cord by MRI and histology. MR images of the spinal cord from animals of the laminectomy, vehicle control, Gal-NS/PC, and GFP-NS/PC groups 3 days after SCI (**A**, sagittal) and 12 weeks after transplantation (**B**, sagittal; **C**, axial). The lesion epicenter appeared as a low-signal-intensity area in the T1WI and as a high-signal-intensity area in the T2WI. **D**: H-E staining. Representative H-E-stained specimens from the laminectomy, vehicle control, Gal-NS/PC, and GFP-NS/PC groups. Scale bars = 1 mm.

GFP, neurofilament 200 kD (NF200; NF200 antibody, 1:1,000 mouse IgG, Chemicon, Temecula, CA), and antimyelin basic protein (MBP; 1:200) was performed.

Grafted NS/PCs that were colabeled with both GFP and cell-type-specific markers were detected with a confocal microscope equipped with an argon-krypton laser (LSM510; Carl Zeiss Co., Oberkochen, Germany) and a fluorescence microscope (Axioskop 2 Plus; Carl Zeiss, Munich, Germany).

Statistical Analysis

A one-way ANOVA followed by the Turkey-Kramer test for multiple comparisons was applied to the behavioral analyses and histological quantifications. All data are shown as the mean ± SEM, with $P < 0.05$ regarded as statistically significant.

RESULTS

Characterization of hNS/PCs In Vitro

To examine the expression of h-galectin-1 in each type of NS/PC (Gal-NS/PCs, GFP-NS/PCs, and naive NS/PCs), we performed Western blotting. The amount of h-galectin-1 in the cell lysate of Gal-NS/PCs was significantly greater than in the lysate of the GFP-NS/PCs or naive NS/PCs (Fig. 1C). Although the amount of h-galectin-1 in the conditioned medium from all the NS/PCs was too small to detect by typical Western blotting, we could detect it in the conditioned medium from all the NS/PCs using the avidin-biotin complex (ABC) method. The amount of h-galectin-1 in the conditioned medium of Gal-NS/PCs was significantly greater than in that of GFP-NS/PCs or naive NS/PCs (data not shown).

We next examined the effect of lentiviral h-galectin-1 transduction on the proliferation and differentiation of NS/PCs. The proliferation rate of each type of NS/PC was quantified by ATP assay. There was no significant difference in the doubling time among the three types of NS/PCs (approximately 150 hr; Fig. 1D).

Gal-NS/PCs, GFP-NS/PCs, and naive NS/PCs differentiated into Tuj1-positive neurons and GFAP-positive astrocytes (Fig. 1E) but not into CNPase-positive oligodendrocytes, 1 week after their differentiation was induced in vitro. Quantitative analysis of their phenotypes revealed no significant differences in the percentages of neurons and astrocytes among the three types of NS/PCs (Fig. 1F).

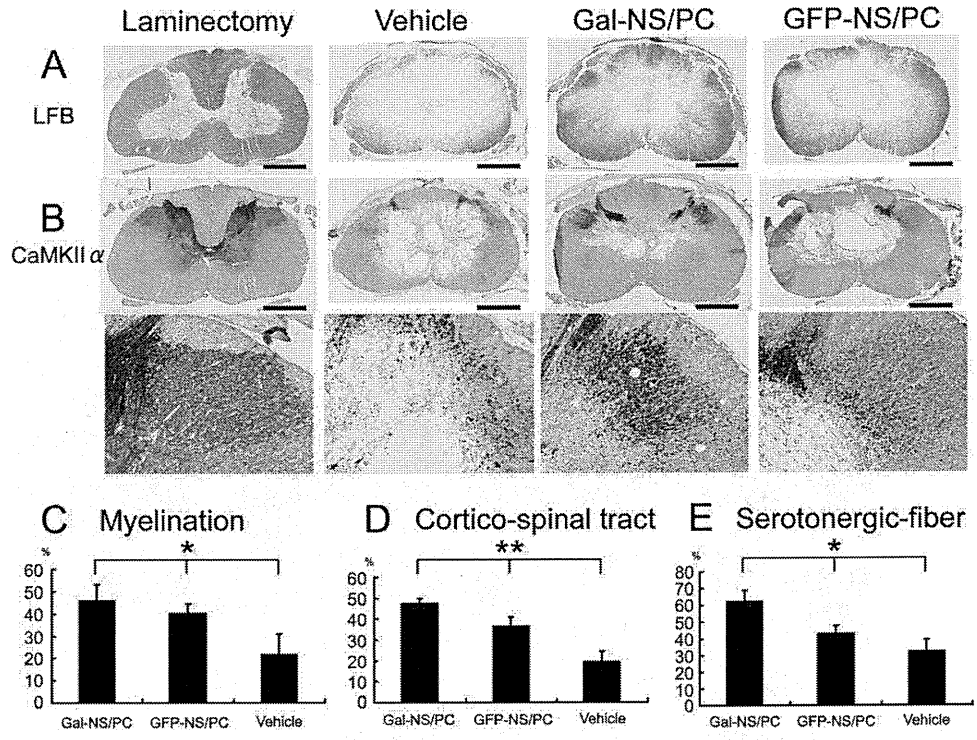

Fig. 3. Myelination, corticospinal fibers, and serotonergic fibers after SCI. Representative axial sections of lesion sites stained with LFB (**A**) and for CaMKIIα (**B**) in the laminectomy, vehicle control, Gal-NS/PC, and GFP-NS/PC groups. Quantification of the LFB$^+$ myelinated (**C**), CaMKIIα$^+$ corticospinal fiber (**D**), and 5HT$^+$ serotonergic fiber (**E**) areas at the lesion site. The percentage of each area relative to the corresponding area in the laminectomy group was calculated using MCID. $*P < 0.05$, $**P < 0.01$. Scale bars = 1 mm.

To determine the effect of lentiviral h-galectin-1 transduction on the neurite growth of each type of NS/PC, the neurite lengths of the neurons derived from Gal-NS/PCs and GFP-NS/PCs were quantified 1 week after their differentiation. The Tuj1/GFP double-positive neurons derived from the Gal-NS/PCs possessed significantly longer neurites than the GFP-NS/PC-derived neurons (Fig. 1G).

Transplantation of Galectin-1-NS/PCs Into the Injured Spinal Cord Reduced the Size of the Lesion Site

In all groups except the laminectomy group, an area of isosignal intensity on the T1-weighted images (T1WI) and a diffuse area of high signal intensity on the T2-weighted images (T2WI) were observed at the lesion epicenter 3 days after the injury, and there was no significant difference in the area of intramedullary T2-high signal among the three groups (Fig. 2A). At 12 weeks after the transplantation, the lesion site appeared as a clearly demarcated low-signal-intensity area on the T1WI and a high-signal-intensity area on the T2WI in all the injury groups, but the lesion appeared smaller in the Gal-NS/PC group than in the GFP-NS/PC and vehicle control groups (Fig. 2B,C). Histological analyses revealed that the intramedullary signal changes observed on the MRI corresponded to the formation of a cavity at the lesion epicenter. The cavity area was smaller in the Gal-NS/PC group than in the GFP-NS/PC and vehicle control groups, which was consistent with the MRI findings (Fig. 2C,D).

Transplantation of Galectin-1 NS/PCs Decreased Demyelination and Increased Corticospinal and Serotonergic Fibers After SCI

Compared with the case in the laminectomy group, the contusive SCI resulted in severe loss of myelin sheath and corticospinal fibers at the lesion site (approximately 20% of the value of the laminectomy group). In both the Gal-NS/PC and the GFP-NS/PC groups, more myelin sheath and corticospinal fibers were observed at the lesion epicenter than in the vehicle control group, and the areas in the Gal-NS/PC group were greater than in the GFP-NS/PC group (Fig. 3A,B). The myelin sheath and corticospinal fibers of the three groups were measured and expressed as a percentage of the corresponding area in the laminectomy group. There were significant differences in the areas of both LFB-positive myelin sheath and α-CaMKII-positive corticospinal fibers among the three groups (Fig. 3C,D).

5HT-positive serotonergic fibers were also lost after SCI at the lesion epicenter. The area of 5HT-positive fibers after injury was approximately 30% of the corresponding area of the laminectomy group. The transplan-

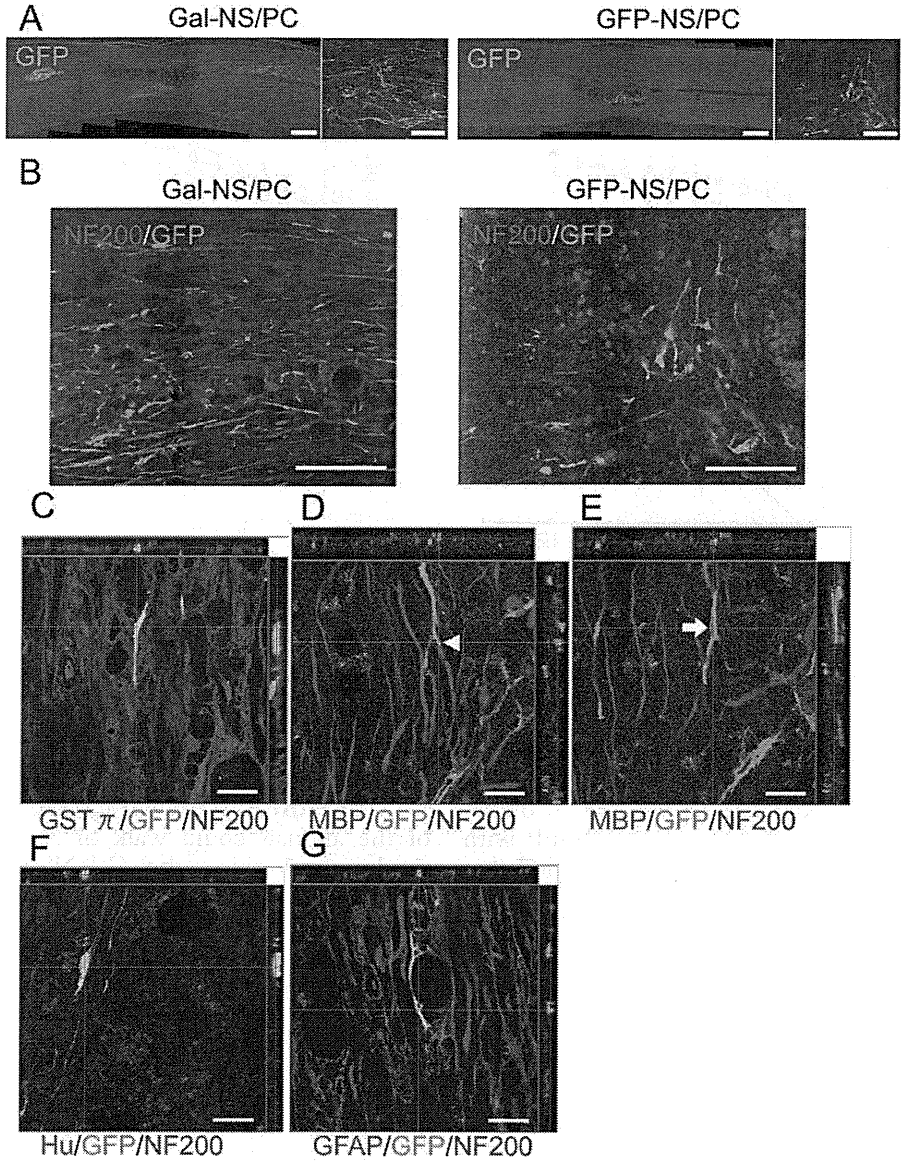

Fig. 4. Grafted human NS/PCs survived and differentiated into oligodendrocytes, neurons, and astrocytes within the injured marmoset spinal cord. **A**: Anti-GFP immunostaining of sagittal sections from the Gal-NS/PC and GFP-NS/PC groups. **B**: Double staining for NF200 and GFP revealed that the differentiated Gal-NS/PC-derived cells possessed longer processes compared with the GFP-NS/PC-derived cells, and these processes were often closely apposed to $NF200^+$ nerve fibers. Confocal images of triple labeling with anti-GFP, anti-GSTpi, and anti-NF200 (**C**) and with anti-GFP, anti-MBP, and anti-NF200 (**D,E**). Grafted Gal-NS/PC-derived oligodendrocytes were closely associated with host neurofilaments (E, arrow) and host myelin sheath (D, arrowhead). Confocal images of triple labeling with anti-GFP, anti-NF200, and anti-Hu (**F**) or anti-GFP, anti-NF200, and anti-GFAP (**G**) revealed that some Gal-NS/PCs also differentiated into neurons or astrocytes. Scale bars = 1 mm at left in A; 50 μm at right in A; 50 μm in B; 20 μm in C–G.

tation of Gal-NS/PCs or GFP-NS/PCs increased the 5HT-positive serotonergic fibers at the epicenter, and the area of serotonergic fibers at the lesion epicenter in the Gal-NS/PC group was greater than in the GFP-NS/PC group (Fig. 3E).

Grafted NS/PCs Survived and Differentiated Into Neurons, Astrocytes, and Oligodendrocytes

To examine the fate of the NS/PCs grafted into the injured spinal cord, fluorescent immunostaining for GFP was performed. In both the Gal-NS/PC and the GFP-NS/PC groups, GFP-positive cells were detected mainly around the cavity (Fig. 4A), but some were distributed as far as 10 mm rostral and caudal to the epicenter, 13 weeks after transplantation. No evidence of tumor formation was observed in either the Gal-NS/PC or the GFP-NS/PC group at 13 weeks after transplantation. Double immunostaining for GFP and NF200 showed that the Gal-NS/PCs possessed longer processes than the GFP-NS/PCs, and these processes were often

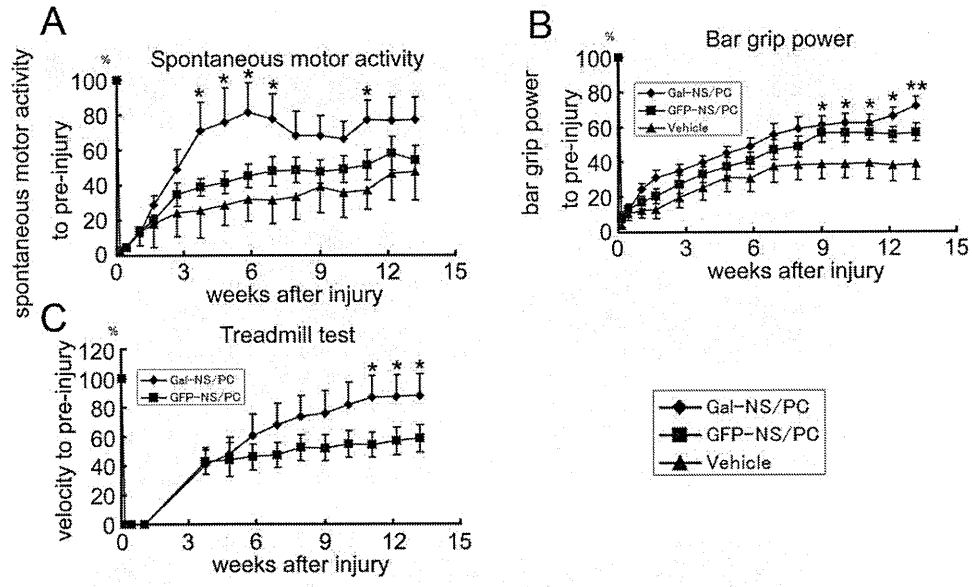

Fig. 5. Behavioral analyses. **A**: Spontaneous motor activity. **B**: Bar grip power. **C**: Treadmill test. The vehicle control group was excluded from the treadmill test, because some animals in the vehicle control group could not walk on the treadmill. $*P < 0.05$, $**P < 0.01$.

aligned with and in close apposition to NF200-positive nerve fibers, which was not observed in the GFP-NS/PC group (Fig. 4B). To examine the phenotype of the transplanted Gal-NS/PCs, double staining for GFP with GSTpi, Hu, or GFAP was performed and revealed that some NS/PCs had differentiated into oligodendrocytes (Fig. 4C), neurons (Fig. 4F), or astrocytes (Fig. 4G). The Gal-NS/PC-derived cells were closely associated with $NF200^+$ fibers (Fig 4E) and MBP^+ myelin sheath (Fig. 4D).

Behavioral Analyses

Spontaneous motor activity. Immediately after injury, the spontaneous motor activity decreased to approximately 0% of the preinjury level, and then increased in all groups. The Gal-NS/PC group showed a rapid increase, reaching a plateau of about 80% by 4 weeks after SCI. The GFP-NS/PC and vehicle control groups showed a more gradual increase. There were significant differences among the three groups by multiple comparisons 4–7 weeks after injury. By 13 weeks after the injury, the motor activities had returned to approximately 80%, 50%, and 40% in the Gal-NS/PC, GFP-NS/PC, and vehicle control groups, respectively (Fig. 5A).

Bar grip power. The maximal grip strength after injury relative to that before injury (percentage grip strength) decreased to approximately 5% in all the groups 1 day after the injury. The grip strength gradually recovered thereafter, reaching a plateau of approximately 70%, 60%, and 40% in the Gal-NS/PC, GFP-NS/PC, and vehicle control groups, respectively. Significant differences in the percentage grip strength were observed among the three groups 9 weeks after injury and thereafter (Fig. 5B).

Treadmill test. Immediately after injury, none of the animals could walk or run by themselves. By 4 weeks after injury, the Gal-NS/PC and GFP-NS/PC groups could walk at approximately 40% of their maximum velocity preinjury (percentage velocity). Because some animals in the vehicle control group could not walk on the treadmill, the vehicle control group was excluded from this analysis. The velocity rapidly recovered to approximately 90% in the Gal-NS/PC group, whereas, in the GFP-NS/PC group, it initially recovered quickly but reached a plateau of approximately 50%. There were significant differences between the Gal-NS/PC and the GFP-NS/PC groups at 10 weeks after SCI and thereafter (Fig. 5C).

DISCUSSION

Stem cell transplantation shows promise as a potential therapy for treating SCI. In particular, ES cells and induced pluripotent stem cells (iPS cells; Takahashi and Yamanaka, 2006) represent possible donor sources for transplantation therapy because of their high pluripotency and potential for proliferation. However, a major problem associated with ES and iPS cell-based therapies is tumor formation (Arnhold et al., 2004; Yoshizaki et al., 2004; Chung et al., 2006; Wernig et al., 2008; Miura et al., 2009), because the grafted cells contain undifferentiated cells even after differentiation is induced. In contrast, no tumor formation has been reported in rodent or primate SCI models subjected to NS/PC-based cell therapy (Ogawa et al., 2002; Ishibashi et al., 2004; Cummings et al., 2005; Iwanami et al., 2005a),

although one recent case report showed brain tumor formation following intracerebellar and intrathecal transplantation of human fetal NS/PCs into an ataxia telangiectasia patient within immune deficiency (Amariglio et al., 2009).

Previous studies (Ogawa et al., 2002; Ishibashi et al., 2004; Cummings et al., 2005; Iwanami et al., 2005a) have shown significant functional recovery after NS/PC transplantation in SCI models, but the improvement has not been sufficient to extrapolate to clinical trials. Therefore, we have been seeking to enhance these effects, by combining hNS/PC transplantation with gene therapy. We showed that galectin-1 applied as an induced gene using a lentiviral vector had neural regenerative effects and improved the recovery of sensorimotor function in an animal model of stroke (Ishibashi et al., 2007).

Lentivirus is broadly used as an ex vivo gene transfer tool for viral gene therapy applications, from basic research to clinical studies (Campbell and Hope, 2005; Young et al., 2006). In fact, several studies have used lentivirus to insert transgenes into NS/PCs (Consiglio et al., 2004; Okada et al., 2005). In the present study, NS/PCs were infected with a recombinant lentivirus carrying h-galectin-1 and also Venus, to track the graft-derived cells in vivo. One advantage of lentivirus is that, unlike retrovirus, which infects dividing cells, nondividing cells can be infected, including most NS/PCs, which divide very slowly (Englund et al., 2000). Another advantage is that, unlike adenovirus, lentivirus can integrate a transgene into the host genome, which prevents dilution of the labeling by cell division. In this study, 80% or more of the NS/PCs were infected with the recombinant lentivirus, and the ratio of the infected cells remained the same after several passages.

One disadvantage of lentivirus is that where and how many copies of reporter genes are inserted into the host genome are uncertain and could affect the cell's phenotype, depending on the site of insertion. Therefore, we compared the proliferation rate and differentiation potential of the Gal-NS/PCs, GFP-NS/PCs, and naive NS/PCs using an ATP doubling time assay and differentiation assay, respectively, and found no significant differences. In addition, there was no significant difference among the Gal-NS/PCs, GFP-NS/PCs, and naive NS/PCs in the differentiation rate of Tuj-1-positive neurons or GFAP-positive astrocytes, consistent with previously reported results (Li et al., 2005; Fig. 1E,F). Thus, there was no change in the differentiation and proliferation rates of the NS/PCs before vs. after lentiviral infection. Furthermore, the proportion of infected cells after several passages was almost constant, and there was no tumor formation for at least 13 weeks after transplantation. Taken together, our findings indicate that the lentivirus infection did not affect the nature of the NS/PCs in any major way.

Galectin-1 has reported functions in a variety of processes, including cell proliferation, differentiation, apoptosis, cell adhesion, metastasis of tumor cells, and inflammation. Galectin-1 is expressed by various stem cells, including embryonic (Ramalho-Santos et al., 2002), neural (Sakaguchi et al., 2006), hematopoietic (Vas et al., 2005), mesenchymal (Silva et al., 2003), and kertinocyte (Tumbar et al., 2004) stem cells. In particular, galectin-1 induced the proliferation of adult NS/PCs in the subventricular zone (SVZ; Sakaguchi et al., 2006) and in hippocampus (Kajitani et al., 2009). Furthermore, in the SVZ, this action was shown to be mediated by galectin-1's carbohydrate-binding activity (Sakaguchi et al., 2006). On the other hand, oxidized galectin-1, which lacks lectin activity, promotes peripheral nerve regeneration (Horie et al., 1999).

In this study, we showed that the neurite growth length of Gal-NS/PC-derived neurons reached 1.5 times that of GFP-NS/PC-derived neurons in vitro, probably because extracellular galectin-1 expressed by the Gal-NS/PCs affected the axonal growth through autocrine and/or paracrine mechanisms similar to those of peripheral nerves (Horie et al., 1999). Therefore, we expected that galectin-1 transfected into NS/PCs would enhance neurite growth in the injured spinal cord.

Our histological analyses revealed that NS/PC transplantation reduced the size of the demyelinated area in the injured spinal cord. Only a residual myelinated area was observed at the outer border of the lesion epicenter in the vehicle control group, whereas, in both the Gal-NS/PC and the GFP-NS/PC groups, more myelin sheath was observed, especially at the anterior and posterior funiculus. In both the Gal-NS/PC and the GFP-NS/PC groups, a much greater area of corticospinal fibers was also observed at the lesion epicenter compared with the vehicle control group. Intriguingly, there was a significantly greater area of corticospinal fibers in the Gal-NS/PC group than in the GFP-NS/PC group. Furthermore, there was a significant difference in the area of the serotonergic fibers, which are closely associated with motor function, among the Gal-NS/PC, GFP-NS/PC, and vehicle control groups.

Both Gal-NS/PCs and GFP-NS/PCs survived and differentiated into neurons, astrocytes, and oligodendrocytes around the cavity. Surviving Gal-NS/PCs were observed up to 10 mm from the transplanted site. The cells that differentiated from the Gal-NS/PCs possessed longer processes than those from GFP-NS/PCs, and these processes were closely apposed to NF200-positive nerve fibers, with some processes enclosing the NF200-positive fibers entirely. It is possible that the processes produced myelin sheath or contributed to the guidance of host-cell axonal growth. These possibilities were supported by the finding that the NF200-positive fibers expressed β1-integrin (data not shown), which is one of the binding proteins for galectin-1 (Moiseeva et al., 2003).

Our results collectively suggest that both Gal-NS/PCs and GFP-NS/PCs supported the regenerative processes of the host spinal cord after injury and that the effect of the Gal-NS/PCs was much greater than that of the GFP-NS/PCs, because of the h-galectin-1 secreted from the transplanted cells. In previous studies, the fol-

lowing mechanisms for the effects of transplanted NS/PCs have been proposed (Horner and Gage, 2000; Okano, 2002b; Schwab, 2002; Okano et al., 2003; Iwanami et al., 2005a). First, immature astrocytes derived from the grafted NS/PCs play an important role in axonal guidance (Hofstetter et al., 2002; Silver and Miller, 2004). Second, the neurons differentiated from the NS/PCs form new synapses with the host neurons, helping to reform the neuronal circuits that had been disrupted by the injury (Ogawa et al., 2002; Okano et al., 2003). Third, trophic effects also improve the survival of the host cells within the injured spinal cord, leading to functional recovery (Namiki et al., 2000; Koda et al., 2002). We believe, based on our finding that Gal-NS/PC-grafted animals showed significantly better functional recovery than GFP-NS/PC-grafted animals at the early phase after transplantation, that the h-galectin-1 produced by the NS/PCs enhanced the third mechanism, although the possibility that Gal-NS/PCs enhanced the effects of the first and second mechanisms cannot be excluded.

It is important to evaluate the cell source for the clinical application to SCI. Accordingly, it will be necessary to compare the merits and demerits of various potential cell sources for the therapeutics of SCI, which include not only NS/PCs but also ES cells (Keirstead et al., 2005), MSCs (Hofstetter et al., 2002), OECs (Li et al., 1997), and nestin-expressing multipotent hair follicle stem cells (Amoh et al., 2005, 2008), from the aspects of safety, effectiveness, and availability.

We previously developed several methods for assessing the motor function of marmosets after SCI, including the measurement of spontaneous motor activity and the bar grip test (Iwanami et al., 2005a,b). Here we observed significant differences between the Gal-NS/PC or the GFP-NS/PC group and the vehicle group in their spontaneous motor activity and bar grip power. However, there was no significant difference between the Gal-NS/PC and the GFP-NS/PC groups when evaluated by these two post hoc tests, because it can be difficult to detect significant differences between mild-injury groups by these evaluations. Therefore, as a new evaluation for motor function to detect the difference between mild-injury groups, we developed a treadmill test. Insofar as the ability to walk or run combines muscle power with coordination of the extremities, this test allows us to discriminate between animals that can run and those that can only walk, a difference that is not recognized by our other evaluation methods. Using this test, we observed significant differences between the Gal-NS/PC and the GFP-NS/PC groups 9–11 weeks after injury.

Intriguingly, significantly greater functional recovery was seen in the Gal-NS/PC group in the spontaneous motor activity and treadmill tests during the early phase, about 5 weeks after injury. This functional improvement might have been due to the greater amounts of LFB-positive myelin sheath, CaMKIIα-positive corticospinal tract, and 5HT-positive serotonergic fibers in the Gal-NS/PC group.

The bar grip power test is used to assess segmental symptoms, mainly involving the motoneurons at the anterior horn. In this study, there was no significant difference in the number of choline acetyltransferase-positive motoneurons at the lesion epicenter, although the Gal-NS/PC group appeared to have more of these cells compared with the GFP-NS/PC and vehicle groups (data not shown). Consistently with this observation, there were no significant differences in the bar grip power during the early phase but significant differences at the late phase, probably because of the compensatory function of the spinal cord to reorganize denervated muscles.

In conclusion, here we have shown that the transplantation of Gal-NS/PCs or GFP-NS/PCs into a primate SCI model improved the recovery of motor functions and that the Gal-NS/PCs had a greater effect than the GFP-NS/PCs. Human NS/PCs expressing h-galectin-1 may therefore have a higher therapeutic potential than control NS/PCs for treating SCI.

ACKNOWLEDGMENTS

We are grateful to Mr. Hajime Ishii, Mr. Kiyoshi Ando, Miss Fumika Toyoda, and Miss Michiko Kamioka for their care of the common marmosets and assistance with the operations.

REFERENCES

Amariglio N, Hirshberg A, Scheithauer BW, Cohen Y, Loewenthal R, Trakhtenbrot L, Paz N, Koren-Michowitz M, Waldman D, Leider-Trejo L, Toren A, Constantini S, Rechavi G. 2009. Donor-derived brain tumor following neural stem cell transplantation in an ataxia telangiectasia patient. PLoS Med 6:e1000029.

Amoh Y, Li L, Campillo R, Kawahara K, Katsuoka K, Penman S, Hoffman RM. 2005. Implanted hair follicle stem cells form Schwann cells that support repair of severed peripheral nerves. Proc Natl Acad Sci U S A 102:17734–17738.

Amoh Y, Li L, Katsuoka K, Hoffman RM. 2008. Multipotent hair follicle stem cells promote repair of spinal cord injury and recovery of walking function. Cell Cycle 7:1865–1869.

Arnhold S, Klein H, Semkova I, Addicks K, Schraermeyer U. 2004. Neurally selected embryonic stem cells induce tumor formation after long-term survival following engraftment into the subretinal space. Invest Ophthalmol Vis Sci 45:4251–4255.

Campbell EM, Hope TJ. 2005. Gene therapy progress and prospects: viral trafficking during infection. Gene Ther 12:1353–1359.

Cao QL, Zhang YP, Howard RM, Walters WM, Tsoulfas P, Whittemore SR. 2001. Pluripotent stem cells engrafted into the normal or lesioned adult rat spinal cord are restricted to a glial lineage. Exp Neurol 167:48–58.

Chung S, Shin BS, Hwang M, Lardaro T, Kang UJ, Isacson O, Kim KS. 2006. Neural precursors derived from embryonic stem cells, but not those from fetal ventral mesencephalon, maintain the potential to differentiate into dopaminergic neurons after expansion in vitro. Stem Cells 24:1583–1593.

Consiglio A, Gritti A, Dolcetta D, Follenzi A, Bordignon C, Gage FH, Vescovi AL, Naldini L. 2004. Robust in vivo gene transfer into adult mammalian neural stem cells by lentiviral vectors. Proc Natl Acad Sci U S A 101:14835–14840.

Cummings BJ, Uchida N, Tamaki SJ, Salazar DL, Hooshmand M, Summers R, Gage FH, Anderson AJ. 2005. Human neural stem cells

differentiate and promote locomotor recovery in spinal cord-injured mice. Proc Natl Acad Sci U S A 102:14069–14074.

David S, Lacroix S. 2003. Molecular approaches to spinal cord repair. Annu Rev Neurosci 26:411–440.

Englund U, Ericson C, Rosenblad C, Mandel RJ, Trono D, Wictorin K, Lundberg C. 2000. The use of a recombinant lentiviral vector for ex vivo gene transfer into the rat CNS. Neuroreport 11:3973–3977.

Hofstetter CP, Schwarz EJ, Hess D, Widenfalk J, El Manira A, Prockop DJ, Olson L. 2002. Marrow stromal cells form guiding strands in the injured spinal cord and promote recovery. Proc Natl Acad Sci U S A 99:2199–2204.

Horie H, Inagaki Y, Sohma Y, Nozawa R, Okawa K, Hasegawa M, Muramatsu N, Kawano H, Horie M, Koyama H, Sakai I, Takeshita K, Kowada Y, Takano M, Kadoya T. 1999. Galectin-1 regulates initial axonal growth in peripheral nerves after axotomy. J Neurosci 19:9964–9974.

Horner PJ, Gage FH. 2000. Regenerating the damaged central nervous system. Nature 407:963–970.

Ishibashi S, Sakaguchi M, Kuroiwa T, Yamasaki M, Kanemura Y, Shizuko I, Shimazaki T, Onodera M, Okano H, Mizusawa H. 2004. Human neural stem/progenitor cells, expanded in long-term neurosphere culture, promote functional recovery after focal ischemia in Mongolian gerbils. J Neurosci Res 78:215–223.

Ishibashi S, Kuroiwa T, Sakaguchi M, Sun L, Kadoya T, Okano H, Mizusawa H. 2007. Galectin-1 regulates neurogenesis in the subventricular zone and promotes functional recovery after stroke. Exp Neurol 207:302–313.

Iwanami A, Kaneko S, Nakamura M, Kanemura Y, Mori H, Kobayashi S, Yamasaki M, Momoshima S, Ishii H, Ando K, Tanioka Y, Tamaoki N, Nomura T, Toyama Y, Okano H. 2005a. Transplantation of human neural stem cells for spinal cord injury in primates. J Neurosci Res 80:182–190.

Iwanami A, Yamane J, Katoh H, Nakamura M, Momoshima S, Ishii H, Tanioka Y, Tamaoki N, Nomura T, Toyama Y, Okano H. 2005b. Establishment of graded spinal cord injury model in a nonhuman primate: the common marmoset. J Neurosci Res 80:172–181.

Johansson CB, Momma S, Clarke DL, Risling M, Lendahl U, Frisen J. 1999. Identification of a neural stem cell in the adult mammalian central nervous system. Cell 96:25–34.

Kajitani K, Nomaru H, Ifuku M, Yutsudo N, Dan Y, Miura T, Tsuchimoto D, Sakumi K, Kadoya T, Horie H, Poirier F, Noda M, Nakabeppu Y. 2009. Galectin-1 promotes basal and kainate-induced proliferation of neural progenitors in the dentate gyrus of adult mouse hippocampus. Cell Death Differ 16:417–427.

Kanemura Y, Mori H, Kobayashi S, Islam O, Kodama E, Yamamoto A, Nakanishi Y, Arita N, Yamasaki M, Okano H, Hara M, Miyake J. 2002. Evaluation of in vitro proliferative activity of human fetal neural stem/progenitor cells using indirect measurements of viable cells based on cellular metabolic activity. J Neurosci Res 69:869–879.

Keirstead HS, Nistor G, Bernal G, Totoiu M, Cloutier F, Sharp K, Steward O. 2005. Human embryonic stem cell-derived oligodendrocyte progenitor cell transplants remyelinate and restore locomotion after spinal cord injury. J Neurosci 25:4694–4705.

Koda M, Murakami M, Ino H, Yoshinaga K, Ikeda O, Hashimoto M, Yamazaki M, Nakayama C, Moriya H. 2002. Brain-derived neurotrophic factor suppresses delayed apoptosis of oligodendrocytes after spinal cord injury in rats. J Neurotrauma 19:777–785.

Li L, Mignone J, Yang M, Matic M, Penman S, Enikolopov G, Hoffman RM. 2003. Nestin expression in hair follicle sheath progenitor cells. Proc Natl Acad Sci U S A 100:9958–9961.

Li X, Xu J, Bai Y, Wang X, Dai X, Liu Y, Zhang J, Zou J, Shen L, Li L. 2005. Isolation and characterization of neural stem cells from human fetal striatum. Biochem Biophys Res Commun 326:425–434.

Li Y, Field PM, Raisman G. 1997. Repair of adult rat corticospinal tract by transplants of olfactory ensheathing cells. Science 277:2000–2002.

Mahanthappa NK, Cooper DN, Barondes SH, Schwarting GA. 1994. Rat olfactory neurons can utilize the endogenous lectin, L-14, in a novel adhesion mechanism. Development 120:1373–1384.

McDonald JW, Liu XZ, Qu Y, Liu S, Mickey SK, Turetsky D, Gottlieb DI, Choi DW. 1999. Transplanted embryonic stem cells survive, differentiate and promote recovery in injured rat spinal cord. Nat Med 5:1410–1412.

Metz GA, Curt A, van de Meent H, Klusman I, Schwab ME, Dietz V. 2000. Validation of the weight-drop contusion model in rats: a comparative study of human spinal cord injury. J Neurotrauma 17:1–17.

Miura K, Okada Y, Aoi T, Okada A, Takahashi K, Okita K, Nakagawa M, Koyanagi M, Tanabe K, Ohnuki M, Ogawa D, Ikeda E, Okano H, Yamanaka S. 2009. Variation in the safety of inducedpluripotent stem cell lines. Nat Biotechnol [July 9 E-pub ahead of print].

Miyoshi H, Blomer U, Takahashi M, Gage FH, Verma IM. 1998. Development of a self-inactivating lentivirus vector. J Virol 72:8150–8157.

Moiseeva EP, Williams B, Goodall AH, Samani NJ. 2003. Galectin-1 interacts with beta-1 subunit of integrin. Biochem Biophys Res Commun 310:1010–1016.

Nagai T, Ibata K, Park ES, Kubota M, Mikoshiba K, Miyawaki A. 2002. A variant of yellow fluorescent protein with fast and efficient maturation for cell-biological applications. Nat Biotechnol 20:87–90.

Nakamura M, Houghtling RA, MacArthur L, Bayer BM, Bregman BS. 2003. Differences in cytokine gene expression profile between acute and secondary injury in adult rat spinal cord. Exp Neurol 184:313–325.

Nakamura M, Okano H, Toyama Y, Dai HN, Finn TP, Bregman BS. 2005. Transplantation of embryonic spinal cord-derived neurospheres support growth of supraspinal projections and functional recovery after spinal cord injury in the neonatal rat. J Neurosci Res 81:457–468.

Namiki J, Kojima A, Tator CH. 2000. Effect of brain-derived neurotrophic factor, nerve growth factor, and neurotrophin-3 on functional recovery and regeneration after spinal cord injury in adult rats. J Neurotrauma 17:1219–1231.

Ogawa Y, Sawamoto K, Miyata T, Miyao S, Watanabe M, Nakamura M, Bregman BS, Koike M, Uchiyama Y, Toyama Y, Okano H. 2002. Transplantation of in vitro-expanded fetal neural progenitor cells results in neurogenesis and functional recovery after spinal cord contusion injury in adult rats. J Neurosci Res 69:925–933.

Ohta K, Fujimura Y, Nakamura M, Watanabe M, Yato Y. 1999. Experimental study on MRI evaluation of the course of cervical spinal cord injury. Spinal Cord 37:580–584.

Okada S, Ishii K, Yamane J, Iwanami A, Ikegami T, Katoh H, Iwamoto Y, Nakamura M, Miyoshi H, Okano HJ, Contag CH, Toyama Y, Okano H. 2005. In vivo imaging of engrafted neural stem cells: its application in evaluating the optimal timing of transplantation for spinal cord injury. FASEB J 19:1839–1841.

Okano H. 2002a. Neural stem cells: progression of basic research and perspective for clinical application. Keio J Med 51:115–128.

Okano H. 2002b. Stem cell biology of the central nervous system. J Neurosci Res 69:698–707.

Okano HJ, Darnell RB. 1997. A hierarchy of Hu RNA binding proteins in developing and adult neurons. J Neurosci 17:3024–3037.

Okano H, Ogawa Y, Nakamura M, Kaneko S, Iwanami A, Toyama Y. 2003. Transplantation of neural stem cells into the spinal cord after injury. Semin Cell Dev Biol 14:191–198.

Olson L. 2002. Medicine: clearing a path for nerve growth. Nature 416:589–590.

Outenreath RL, Jones AL. 1992. Influence of an endogenous lectin substrate on cultured dorsal root ganglion cells. J Neurocytol 21:788–795.

Perillo NL, Pace KE, Seilhamer JJ, Baum LG. 1995. Apoptosis of T cells mediated by galectin-1. Nature 378:736–739.

Perillo NL, Marcus ME, Baum LG. 1998. Galectins: versatile modulators of cell adhesion, cell proliferation, and cell death. J Mol Med 76:402–412.

Puche AC, Poirier F, Hair M, Bartlett PF, Key B. 1996. Role of galectin-1 in the developing mouse olfactory system. Dev Biol 179:274–287.

Rabinovich GA, Alonso CR, Sotomayor CE, Durand S, Bocco JL, Riera CM. 2000a. Molecular mechanisms implicated in galectin-1-induced apoptosis: activation of the AP-1 transcription factor and downregulation of Bcl-2. Cell Death Differ 7:747–753.

Rabinovich GA, Sotomayor CE, Riera CM, Bianco I, Correa SG. 2000b. Evidence of a role for galectin-1 in acute inflammation. Eur J Immunol 30:1331–1339.

Rabinovich GA, Baum LG, Tinari N, Paganelli R, Natoli C, Liu FT, Iacobelli S. 2002. Galectins and their ligands: amplifiers, silencers or tuners of the inflammatory response? Trends Immunol 23:313–320.

Ramalho-Santos M, Yoon S, Matsuzaki Y, Mulligan RC, Melton DA. 2002. "Stemness": transcriptional profiling of embryonic and adult stem cells. Science 298:597–600.

Reynolds BA, Weiss S. 1996. Clonal and population analyses demonstrate that an EGF-responsive mammalian embryonic CNS precursor is a stem cell. Dev Biol 175:1–13.

Sakaguchi M, Shingo T, Shimazaki T, Okano HJ, Shiwa M, Ishibashi S, Oguro H, Ninomiya M, Kadoya T, Horie H, Shibuya A, Mizusawa H, Poirier F, Nakauchi H, Sawamoto K, Okano H. 2006. A carbohydrate-binding protein, galectin-1, promotes proliferation of adult neural stem cells. Proc Natl Acad Sci U S A 103:7112–7117.

Schwab ME. 2002. Repairing the injured spinal cord. Science 295:1029–1031.

Silva WA Jr, Covas DT, Panepucci RA, Proto-Siqueira R, Siufi JL, Zanette DL, Santos AR, Zago MA. 2003. The profile of gene expression of human marrow mesenchymal stem cells. Stem Cells 21:661–669.

Silver J, Miller JH. 2004. Regeneration beyond the glial scar. Nat Rev Neurosci 5:146–156.

Takahashi K, Yamanaka S. 2006. Induction of pluripotent stem cells from mouse embryonic and adult fibroblast cultures by defined factors. Cell 126:663–676.

Tumbar T, Guasch G, Greco V, Blanpain C, Lowry WE, Rendl M, Fuchs E. 2004. Defining the epithelial stem cell niche in skin. Science 303:359–363.

Vas V, Fajka-Boja R, Ion G, Dudics V, Monostori E, Uher F. 2005. Biphasic effect of recombinant galectin-1 on the growth and death of early hematopoietic cells. Stem Cells 23:279–287.

Wernig M, Zhao JP, Pruszak J, Hedlund E, Fu D, Soldner F, Broccoli V, Constantine-Paton M, Isacson O, Jaenisch R. 2008. Neurons derived from reprogrammed fibroblasts functionally integrate into the fetal brain and improve symptoms of rats with Parkinson's disease. Proc Natl Acad Sci U S A 105:5856–5861.

Widenfalk J, Lundstromer K, Jubran M, Brene S, Olson L. 2001. Neurotrophic factors and receptors in the immature and adult spinal cord after mechanical injury or kainic acid. J Neurosci 21:3457–3475.

Yoshizaki T, Inaji M, Kouike H, Shimazaki T, Sawamoto K, Ando K, Date I, Kobayashi K, Suhara T, Uchiyama Y, Okano H. 2004. Isolation and transplantation of dopaminergic neurons generated from mouse embryonic stem cells. Neurosci Lett 363:33–37.

Young LS, Searle PF, Onion D, Mautner V. 2006. Viral gene therapy strategies: from basic science to clinical application. J Pathol 208:299–318.